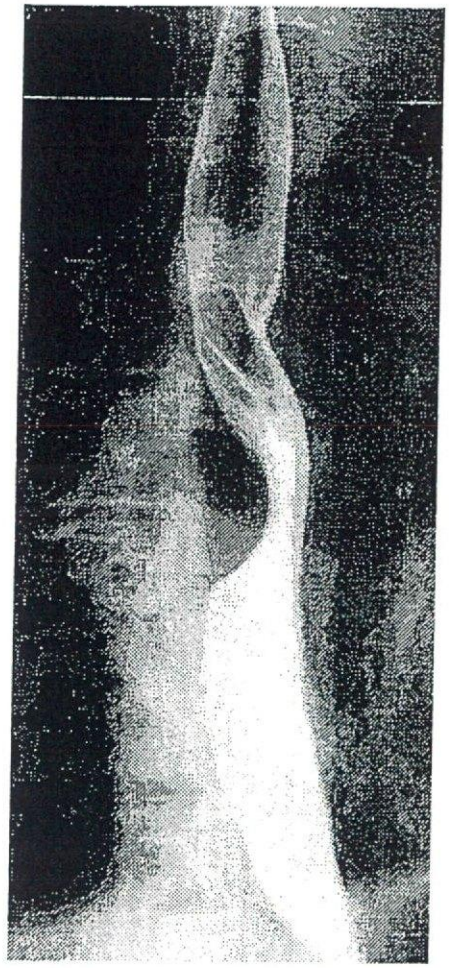

Fig. 1 A protruding tumor with a smooth surface is detected in the middle thoracic esophagus.

mediastinal pleura (Fig. 3A). The pleura was incised over the lesion, the esophageal longitudinal muscle was incised at the midpoint of the tumor, and the white tumor was exposed (Fig. 3B). The tumor was then enucleated by careful dissection using a Kodama Di-suction (Sumitomo Bakelite Co., Ltd, Nagoya, Japan; Fig. 3C). A few blood vessels fed the tumor, and they were cut using a coagulation shear. Following removal of the tumor, an endoscope was orally inserted into the esophagus and no injury to the esophageal mucosa was detected. In addition, no air-bubble infused into the esophagus from the endoscopy was detected in the thorax. The esophageal muscle layer was closed longitudinally using absorbal sutures. The tumor was inserted into a bag and extracted through the port site slightly expanded to 2.5 cm (Fig. 3D). The patient's course was uneventful after surgery.

Macroscopically, the enucleated tumor was white, $4.5 \times 3.3 \times 2.5$ cm in size, and showed neither bleeding nor necrotic tissue. Histopathologically, dense, elongated spindle-shaped tumor cells with a dense chromatin nucleus and basophilic cytoplasm were observed (Fig. 4A). The mitotic figures were hardly observed in the tumor cells. In immunohistochemistry, almost all the tumor cells were positive for CD34 and CD117 (c-kit protein) antigens while these cells were negative for S-100 protein and a-smooth muscle actin (Fig. 4B–E). From these findings, the tumor was diagnosed as GIST of the esophagus. The Ki-67 positive ratio of the tumor nuclei (labeling index) was about 0.5% (Fig. 4F).

DISCUSSION

GIST is a rare entity of the esophagus. Previously, many patients with a leiomyoma of the esophagus have been reported,[2,3] however, esophageal stromal tumor with CD34 and CD117 coexpression, which is considered to be GIST, is rare.[1] Recently, the concept of GIST has been accepted histopathologically and clinicopathologically in mesenchymal tumors, and

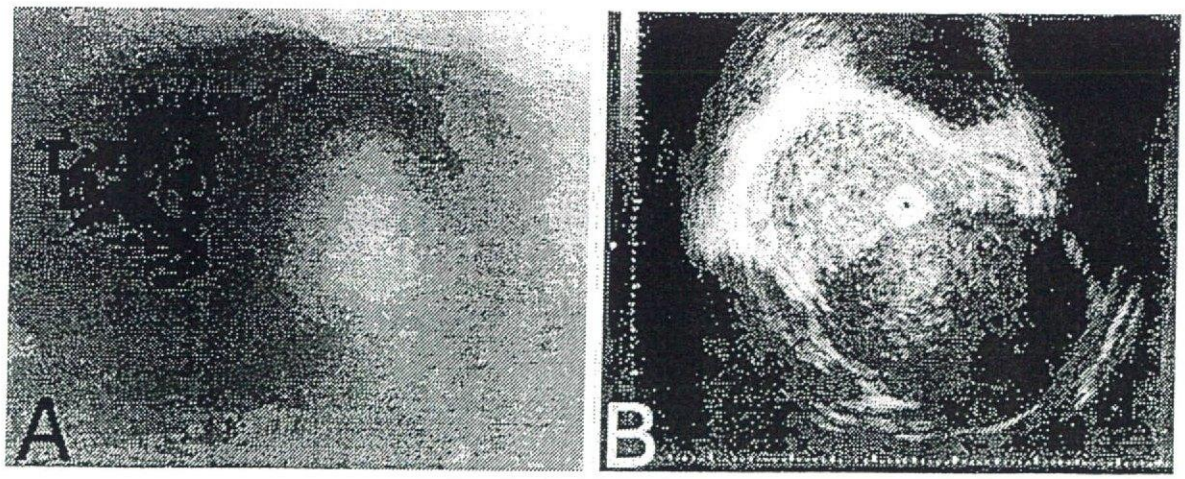

Fig. 2 Endoscopic examination: (A) esophagoscopy shows a submucosal lesion covered with normal esophageal mucosa; (B) endoscopic ultrasonogram shows a submucosal tumor continuing with the proper muscle layer of the esophagus.

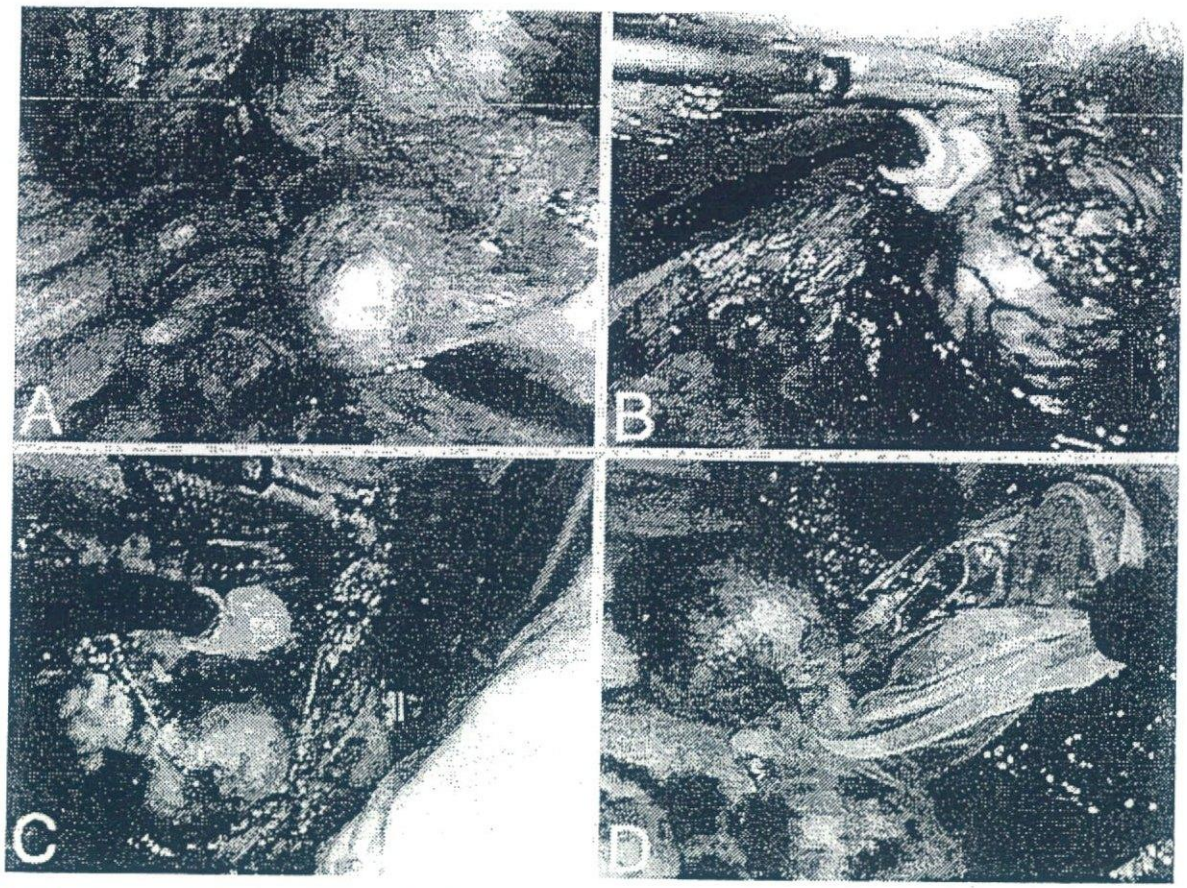

Fig. 3 Thoracoscopic findings: (A) the esophageal tumor projects into the right thoracic space; (B) the white submucosal tumor is exposed in the proper muscle layer of the esophagus; (C) the tumor is enucleated with a Kodama Di-suction (a useful instrument for dissection of the tumor and as a sucker); (D) the enucleated tumor is collected in a bag.

GIST is considered separate from myogenic or neurogenic mesenchymal tumor of the GI tract.[4,5] Miettinen *et al.* first documented and analyzed GIST of the esophagus, and histologically distinguished them from leiomyomas and leiomyosarcomas.[1] In the present case, the lesion was endoscopically a submucosal tumor of the esophagus, and judged to have originated from the proper muscle layer by EUS before surgery. Histopathologically, the removed esophageal tumor revealed a high cellularity of spindle cells with neither reaction for a smooth muscle actin nor S-100 protein but with positive reactions for both CD34 and CD117. These clinicopathologic findings showed that this esophageal submucosal tumor was a GIST.

GIST has a malignant potential.[6] Patients with a large GIST are associated with a poor prognosis, and surgical treatment for these patients is controversial.[7] Laparoscopic surgery has been widely available for patients with a small GIST, and these patients show a good prognosis. In esophageal stromal tumor, Miettinen *et al.* reported that nine of 17 patients with esophageal GIST died of the disease,[1] although surgical treatment was not analyzed and discussed in these patients. All patients who died of the disease had a large GIST between 5 cm and 25 cm in size. In esophageal GIST, tumor size may be important for surgical management and patient prognosis. In the present case, because the tumor enlarged over 11 months on EUS and the patient had dysphagia, the tumor was enucleated. Fortunately, the enucleated GIST was 4.5 cm in diameter, and showed histopathologically low mitosis and low Ki-67 labeling index.

For esophageal leiomyomas, several surgical or endoscopic approaches have been reported. The traditional method using thoracotomy was associated with high surgical stress and invasiveness. Several thoracoscopic procedures have recently been applied for benign esophageal disorders including esophageal leiomyomas.[8,9] For surgical treatment of esophageal submucosal tumors, the thoracoscopic approach showed many benefits including minimal scarring, decreased pain and rapid recovery after surgery.[8–10] The management and technique of thoracoscopic surgery in this patient with GIST was similar to those of previous studies of esophageal leiomyoma. In this situation, perforation of the

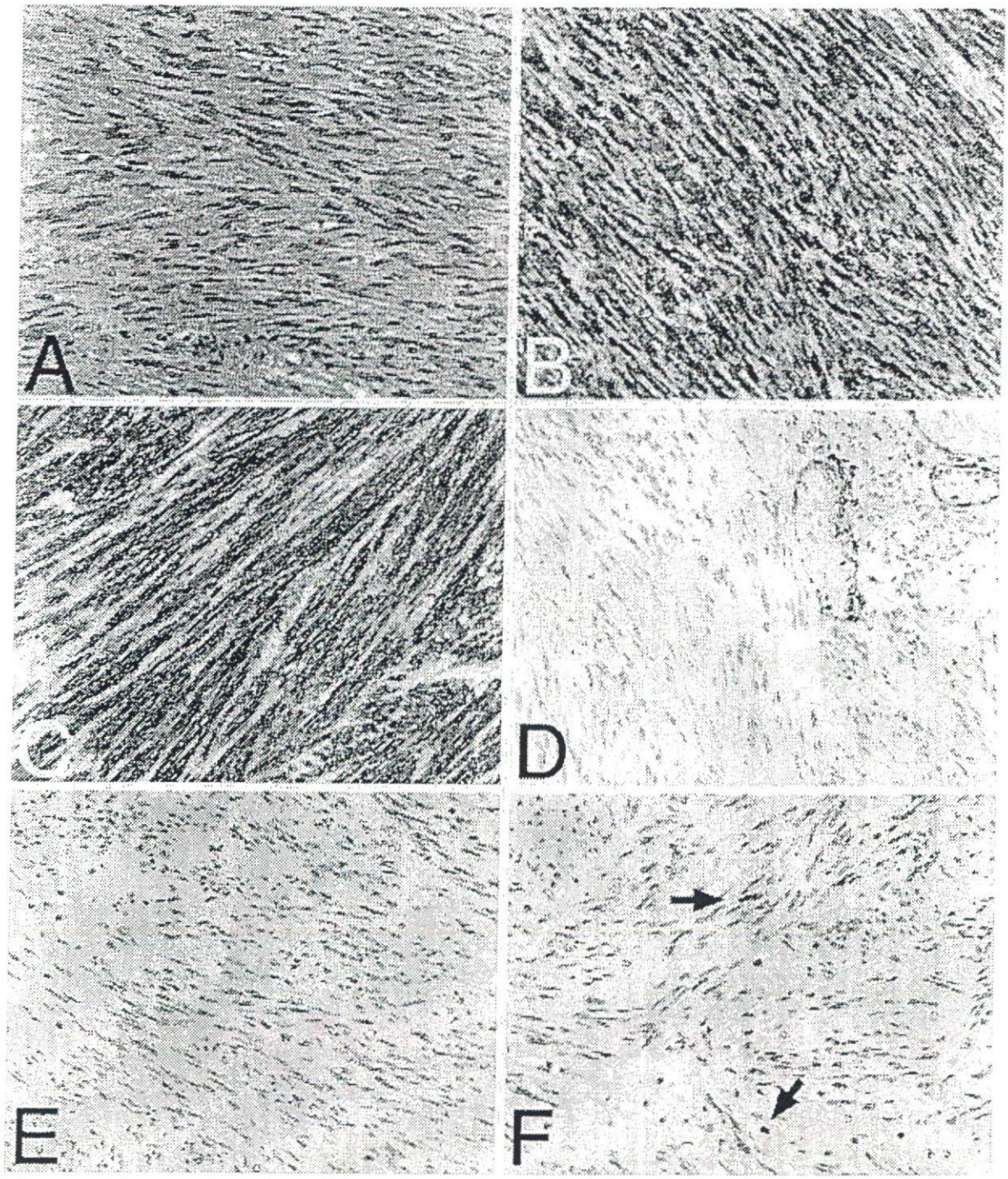

Fig. 4 Histopathologic findings: (A) HE staining; (B) CD 34 immunostaining; (C) CD 117 immunostaining; (D) α-smooth muscle actin immunostaining; (E) S-100 protein immunostaining; (F) Ki-67 immunostaining. The spindle-shaped tumor cells showed a positive reaction for CD 34 and CD 117 antigens, but no reaction for α-smooth muscle actin or S-100 protein. Ki-67 immunostaining produced a positive in the nuclei of the tumor cells (arrowed).

esophagus may be the most common complication developing from dangerous complications such as leakage and abscesses in the mediastinum and the thorax.[9] In previous studies of esophageal leiomyoma, an enucleation of the tumor was performed using a mounted swab or a coagulation shear. In the present case, we used the Kodama Di-suction thoracoscopically for the removal and enucleation of the esophageal stromal tumor.[11] Although this GIST was fed by several blood vessels and these vessels were cut using the coagulation shear, the Kodama Di-suction, which functions as both a

dissector and a sucker, may be useful for the enucleation of submucosal tumors because there was no injury of the esophageal mucosa in the present case.

References

1 Miettinen M, Sarlomo-Rikala M, Sobin L H, Lasota J. Esophageal stromal tumors. A clinicopathologic, immunohistochemical, and molecular genetic study of 17 cases and comparison with esophageal leiomyomas and leiomyosarcomas. Am J Surg Pathol 2000; 24: 211–22.

2 Miettinen M. Gastrointestinal stromal tumors. An immunohistochemical study of cellular differentiation. Am J Clin Pathol 1988; 89: 601–10.

3 Ueyama T, Guo K-J, Hashimoto H, Daimaru Y, Enjoji M. A clinicopathologic and immunohistochemical study of gastrointestinal stromal tumors. Cancer 1992; 69: 947–55.

4 Monihan J M, Carr N J, Sobin L H. CD34 immunoexpression in stromal tumors of the gastrointestinal tract and in mesenteric fibromatoses. Histopathology 1994; 25: 469–73.

5 Miettinen M, Virolainen M, Sarlomo-Rikala M. Gastrointestinal stromal tumors – value of CD34 antigen in their identification and separation from true leiomyomas and schwanomas. Am J Surg Pathol 1995; 19: 207–16.

6 Franquemont D W. Differentiation and risk assessment of gastrointestinal stromal tumors. Am J Clin Pathol 1995; 103: 41–7.

7 DeMatteo R P, Lewis J J, Leung D, Mudan S S, Woodruff J M, Brennan M F. Two hundred gastrointestinal stromal tumors. Recurrence patterns and prognostic factors for survival. Ann Surg 2000; 231: 51–8.

8 Everitt N J, Glinatsis M, McMahon M J. Thoracoscopic enucleation of leiomyoma of the oesophagus. Br J Surg 1992; 79: 643.

9 Gossot D, Fourquier P, El Meteini M, Celerier M. Technical aspects of endoscopic removal of benign tumors of the esophagus. Surg Endosc 1993; 7: 102–3.

10 Bardini R, Segalin A, Ruol A, Pavanello M, Peracchia A. Videothoracoscopic enucleation of esophageal leiomyoma. Ann Thorac Surg 1992; 54: 576–7.

11 Kondo K, Naito H, Adachi H, Takahashi H. [Video-assisted thoracic surgery for mediastinal neuroblastoma.] J Jpn Soc Endosc Surg (Nihon Naishikyougeka Gakkaizasshi) 1999; 4: 525–9. (In Japanese.)

HELICOBACTER

Roles of *virD4* and *cagG* genes in the *cag* pathogenicity island of *Helicobacter pylori* using a Mongolian gerbil model

H Saito, Y Yamaoka, S Ishizone, F Maruta, A Sugiyama, D Y Graham, K Yamauchi, H Ota, S Miyagawa

Gut 2005;**54**:584–590. doi: 10.1136/gut.2004.058982

See end of article for authors' affiliations

Correspondence to: Dr Y Yamaoka, Michael E DeBakey Veterans Affairs Medical Center (111D), Rm 3A-320, 200 Holcombe Blvd, Houston, TX 77030, USA; yyamaoka@bcm.tmc.edu

Revised version received 23 December 2004
Accepted for publication 10 January 2005

Background and Aims: The roles of the *virD4* and the *cagG* genes in the *cag* pathogenicity island of *Helicobacter pylori* for gastroduodenal pathogenesis are unclear and their roles in vivo have not been examined.

Methods: Seven week old male Mongolian gerbils were inoculated with the wild type *H pylori* TN2GF4, its isogenic *virD4*, or *cagG* mutants. Animals were sacrificed at 4, 12, and 24 weeks after inoculation. Gastric inflammation and *H pylori* density were evaluated by histology, inflammatory response (as measured by interleukin (IL)-1β mRNA levels), proliferative activity (as assessed by 5′-bromo-2′deoxyuridine labelling indices), and host systemic reaction (as measured by anti-*H pylori* IgG antibody).

Results: Degree of gastric inflammation, proliferative activity, and mucosal IL-1β mRNA levels remained low throughout the first 12 weeks in gerbils infected with the *virD4* mutants. Degree of gastric inflammation and proliferative activity increased at 24 weeks with the *virD4* mutants reaching levels comparative with those seen at four weeks with the wild-type strains. Mucosal IL-1β mRNA levels were also increased at 24 weeks with the *virD4* mutants and levels at 24 weeks were similar between the wild-type and *virD4* mutants. In contrast, gerbils infected with the *cagG* mutants had reduced ability to colonise gerbils, and no or little gastric inflammation or proliferative activity was observed.

Conclusions: Loss of the *virD4* gene temporally retarded but did not abrogate gastric inflammation. Loss of the *cagG* gene abolished gastric inflammation partially via reduced ability to colonise gerbils. Unknown factors related to the type IV secretion system other than CagA may influence gastric inflammation.

The presence of the *cag* pathogenicity island (PAI) in *Helicobacter pylori* is associated with increased mucosal inflammation and an increased risk of the development of gastric cancer or peptic ulcer disease.[1–4] The *cag* PAI is a 40 kbp cluster of approximately 27 genes that encodes a type IV secretary apparatus (a molecular syringe) which injects the CagA protein and possibly other unknown proteins into eukaryotic cells.[5–11] Defining the roles of the various genes in the *cag* PAI in the pathogenesis of *H pylori* related diseases is an area of active research interest. In vitro experiments using gastric cancer cells cocultured with *H pylori* indicate that several genes in the island are involved in induction of a proinflammatory cytokine; interleukin (IL)-8 (for example, *cagE* but not *cagA*).[3 12] IL-8 is a potent neutrophil chemotactic and activating peptide produced by gastric epithelial cells and is thought to play a major role in the pathogenesis of *H pylori* associated diseases. Recent in vivo studies using Mongolian gerbils (*Meriones unguiculatus*) showed that *cagE* knockout mutants were associated with reduced gastric inflammation[13–15] and did not induce gastric ulcers or gastric cancer.[14] In contrast, *cagA* knockout mutants caused gastric inflammation similar to the parental strain.[16] The in vivo function of other genes in the *cag* PAI has not been examined. This study therefore involves two genes in the *cag* PAI (*virD4* and *cagG*), both of which have been suggested to play unique roles based on in vitro studies,[12 17 18 19] but their roles in vivo have not been examined.

virD4 (*hp0524*; *hp* number from GenBank: AE000511) is one of seven genes in the *cag* PAI that are virulent (*vir*) gene homologues.[20] *virD4* is a key component of the type IV secretion system. In the plant pathogen *Agrobacterium tumefaciens*, VirD4 is thought to mediate introduction of the nucleoprotein complex into the transporter by an energy dependent mechanism.[11 21] In *H pylori*, VirD4 is thought to act as an adapter protein for the transfer of CagA protein and possibly other unknown proteins into the transfer channel formed by other Vir proteins in the *cag* PAI.[17] This is based on previous reports showing that knockout of the *virD4* gene resulted in loss of CagA translocation/phosphorylation as well as loss of *H pylori* induced host cytoskeletal rearrangement.[17] Although the role of VirD4 in relation to IL-8 secretion from host cells remains unclear,[12 17 18] the consensus is that loss of VirD4 does not parallel the reduction in IL-8 in contrast with other Vir factors in the *cag* PAI.

The second gene we examined was the *cagG* gene which is not a *vir* homologue gene but has weak homology to the flagellar motor switch protein gene or toxin coregulated pilus biosynthesis protein gene.[3 20] The *cagG* gene has recently been reported to be involved in adherence to gastric epithelial cells.[19] As the roles of these two gene have not been investigated in vivo, we used the Mongolian gerbil model to examine their functions in vivo in relation to gastric mucosal inflammation.

MATERIALS AND METHODS

Bacterial strains

We used a clinical isolate of *H pylori* strain TN2GF4 (kind gift from Masafumi Nakao, Takeda Chemical Industries Ltd,

Abbreviations: AI, arbitrary index; BrdU, 5′-bromo-2′deoxyuridine; CFU, colony forming units; GAPDH, glyceraldehyde-3-phosphate dehydrogenase; IL, interleukin; MNC, mononuclear cells; PAI, pathogenicity island; PCR, polymerase chain reaction; PMN, polymorphonuclear cells, RT, reverse transcription; vir, virulent

www.gutjnl.com

Osaka, Japan) and its isogenic knockout mutants for *cagG* and *virD4*. Strain TN2GF4 was isolated from Japanese gastric ulcer patients and is reported to induce gastric ulcer and gastric cancer in gerbils over 62 weeks.[13]

Isogenic mutant strains were constructed from a single colony from stock frozen *H pylori*. A portion of the genes encoding the *cagG* and *virD4* genes was amplified by polymerase chain reaction (PCR) and the amplified fragment was inserted into the *Eco*RV restriction enzyme site of pBluescriptSK+ (Stratagene, La Jolla, California, USA). A chloramphenicol resistance gene cassette (a gift from DE Taylor, University of Alberta, Edmonton, Canada) was inserted into *Bsm*I and *Hind*III sites of the insert DNA for the *cagG* and *virD4* genes, respectively. All plasmids (1–2 μg) were used for inactivation of chromosomal genes by natural transformation, as previously described.[22] Inactivation of the genes was confirmed by PCR amplification followed by Southern blot hybridisation.

IL-8 levels from gastric cancer cells cocultured with *H pylori*

In vitro IL-8 measurement was performed as previously described.[23] Briefly, the human gastric cell line MKN 45 (Japanese Cancer Research Bank, Tsukuba, Japan) (1×10^5/ml) was plated onto 24 well plates and cultured for two days. *H pylori* was added to the cultured cells (bacterium to cell ratio of 100:1) and incubated for 24 hours. IL-8 in the supernatant was measured by an enzyme linked immunosorbent assay (R&D Systems, Minneapolis, Minnesota, USA) in triplicate.

Animal, housing, and H pylori challenge

Specific pathogen free seven week old male Mongolian gerbils (MGS/Sea; Seac Yoshitomi, Fukuoka, Japan) were used in this study. They were housed in an air conditioned biohazard room designed for infectious animals, with a 12 hour light/12 hour dark cycle. They were provided with a rodent diet and water ad libitum. All experimental protocols were approved by the Animal Experiment Committee of Shinshu University School of Medicine, Matsumoto, Japan.

H pylori were grown in Brucella broth supplemented with 10% (vol/vol) horse serum for 40 hours at 37℃ under microaerobic conditions and saturated humidity, with shaking at 150 rpm. After fasting for 24 hours, each animal was orogastrically inoculated with 1.0 ml of an inoculum preparation of *H pylori* (10^8 colony forming units (CFU)/ml) or sterile Brucella broth (as an uninfected control) using gastric intubation needles. No specific pretreatments (for example, acid inhibition or antibiotics) were used before orogastric *H pylori* inoculation. Four hours after administration, animals were again allowed free access to water and food.

Time course and euthanasia

Mongolian gerbils were assigned to one of three groups: inoculated with the wild-type *H pylori* strains, with its *cagG* mutants, or with its *virD4* mutants. Infected gerbils were killed and underwent necropsy at 4, 12, and 24 weeks after *H pylori* inoculation. Eight to nine gerbils were used for each time point. Uninfected control gerbils were killed at 11, 19, and 31 weeks of age (to serve as controls for the infected animals 4, 12, and 24 weeks after *H pylori* inoculation) (n = 6 each). Thirty minutes before being killed, gerbils were given 200 mg/kg of 5′-bromo-2′deoxyuridine (BrdU) intraperitoneally.

At necropsy, stomachs were opened along the greater curvature, beginning at the gastro-oesophageal junction and ending at the proximal portion of the duodenum, and observed macroscopically. Stomachs were then divided longitudinally into two parts and one half was fixed in 20% phosphate buffered formalin fixative for histological examination. The other part was further divided into the pyloric gland mucosa (antrum) and the fundic gland mucosa (corpus). The gastric mucosa was separated as much as possible from the underlying muscle using sharp dissection. Each specimen was placed on dry ice and stored at −80℃ for cytokines mRNA analysis.

Table 1 Primers and probes used in this study

GAPDH	
Forward:	5′- CATGGCCTTCCGAGTTCCT-3′
Reverse:	5′-TTCTGCAGTCGGCATGTCA-3′
Probe:	5′-VIC-CCCCCAACGTGTCTGTCGTGGA-TAMURA-3′
IL-1β	
Forward:	5′-GGTGACACAAGCAGCAACAAA-3′
Reverse:	5′-CATCACACAGGACAGGTACAGATTCT -3′
Probe:	5′-FAM-TACCGGTGGCCTTGGGCCTCA-TAMURA-3′

GAPDH, glyceraldehyde-3-phosphate dehydrogenase; IL, interleukin; FAM, 6-carboxyfluorescein; TAMURA, 6-carboxy-N, N, N′, N′-tetramethylrhodamine.

H pylori cultures

A 1 mm^2 piece of gastric mucosa from the pyloric part of the stomach was used for culture of *H pylori*. These fragments were minced with Brucella broth and several diluted aliquots were spread on commercially available *H pylori* selective agar plates (Eiken Chemical Co., Tokyo, Japan). Cultures were incubated for seven days and the number of *H pylori* colonies per plate was counted.

Histological examination

Half of the stomach was stapled onto paper and fixed in 20% phosphate buffered formalin for 24 hours at 4℃. The fixed gastric tissue was processed for histopathological examination, and paraffin embedded sections were sliced and stained with haematoxylin-eosin or May-Grunwald-Giemsa. The degree of inflammation was graded according to the updated Sydney system.[24]

Analysis of IL-1β mRNA expression by real time quantitative PCR

Total RNA was extracted from the gastric mucosa using an RNA extraction kit (Isogen; Nippon Gene, Tokyo, Japan). After DNase treatment, 5 μg of total RNA were subjected to reverse transcription (RT) using 200 U of Moloney murine leukaemia virus reverse transcriptase (Life Technologies, Inc., Gaithersburg, Maryland, USA). Partial gerbil specific IL-1β cDNA sequences were recently cloned in our group (GenBank accession number AB164705) and we normalised IL-1β mRNA levels to the gerbil specific glyceraldehyde-3-phosphate dehydrogenase (GAPDH) mRNA identified previously.[13] Specific primers and TaqMan probes are listed in table 1. Real time PCR was performed using an ABI Prism 7700 Sequence-Detection System (Perkin-Elmer Applied Biosystems) at 50℃ for two minutes, 95℃ for 10 minutes, followed by 50 cycles of 95℃ for 15 seconds and 60℃ for 60 seconds. IL-1β mRNA levels were expressed as the ratio of IL-1β mRNA to GAPDH mRNA (100 000 × IL-1β mRNA (unit/μl)/GAPDH mRNA (unit/μl)). Each assay was performed in triplicate.

Serology

Before the animals were killed, blood samples were obtained from the orbital plexus using haematocrit tubes. Sera were used to measure the titre of anti-*H pylori* IgG antibody, as previously described.[25 26] Antibody titre was expressed as an arbitrary index (AI) with values greater than 1.37

Table 2 Prevalence of *H pylori* colonisation in gerbils evaluated with different methods

	Wild-type			*cagG* mutants			*virD4* mutants		
	4W (n=8)	12W (n=8)	24W (n=8)	4W (n=8)	12W (n=8)	24W (n=9)	4W (n=8)	12W (n=8)	24W (n=9)
Culture (pyloric)	88%	100%	88%	0%	75%	11%	25%	88%	100%
Serology	75%	100%	100%	13%	0%	22%	100%	100%	100%
Histology (pyloric)	100%	100%	100%	38%	88%	100%	100%	75%	100%
Histology (fundic)	100%	100%	100%	38%	88%	89%	88%	88%	100%
Colonisation (total)	100%	100%	100%	38%	100%	100%	100%	100%	100%

W, weeks post infection.
Gerbils were classified as *H pylori* positive if culture and/or histology yielded positive results.

(≤15 weeks of age) or 1.90 (>15 weeks) being scored as positive for *H pylori* based on our system.[26]

Statistical analyses

Results are presented as medians when the data were not distributed normally, and mean (SEM) when they were. Statistical analyses included the Student's *t* test or the Mann-Whitney rank sum test, depending on whether the data were normally distributed. Prevalence of infection was analysed using Fisher's extract test. A p value of <0.05 was considered significant.

RESULTS

In vitro IL-8 production from MKN45 cells cocultured with *H pylori*

The wild-type strain (TN2GF4) containing a complete set of the *cag* PAI genes induced greater secretion of IL-8 from MKN45 cells (mean (SEM) 3162 (147) pg/ml) than the *virD4* mutants (2318 (43) pg/ml) ($p<0.01$) or the *cagG* mutants (325 (9) pg/ml) ($p<0.001$). In agreement with reports by Selbach and colleagues,[17] the *virD4* knockout mutants induced intermediate levels of IL-8 whereas the *cagG* mutants induced less than one tenth of IL-8 produced by the wild-type strain (control IL-8 levels without *H pylori* infection were 113 (5) pg/ml).

Establishment of *H pylori* infection in Mongolian gerbils

Ninety two gerbils were used. Bacteriological, histological, and serological examination showed no detectable *H pylori* in control gerbils. Infection status in inoculated gerbils was assessed using bacteriological and histological examination (table 2). Gerbils were classified as *H pylori* positive if culture and/or histology yielded positive results. With the exception of five gerbils infected with the *cagG* mutants for four weeks, all gerbils were successfully infected (table 2). The five gerbils with failed infection were excluded from further analyses.

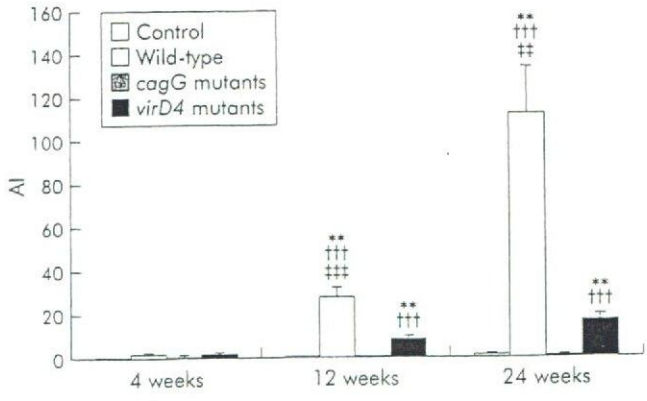

Figure 1 Titre of serum anti-*Helicobacter pylori* IgG antibodies of Mongolian gerbils inoculated orally with *H pylori* or without *H pylori* infection (control). Mean (SEM) values are presented. **p<0.01 compared with control; †††p<0.001 compared with the *cagG* knockout mutants; ‡‡p<0.01, ‡‡‡p<0.001 compared with the *virD4* knockout mutants. AI, arbitrary index.

H pylori IgG antibody titres were significantly increased in gerbils inoculated with the wild-type strains at 12 and 24 weeks compared with those at four weeks (27.9 (4.3) at 12 weeks and 111.9 (21.7) at 24 weeks compared with 2.2 (0.3) at four weeks) ($p<0.001$ for each) (fig 1). Although seroconversion occurred in all gerbils inoculated with the *virD4* mutants, antibody titres were significantly lower than those of gerbils infected with the wild-type strains (8.6 (1.2) at 12 weeks and 17.0 (3.1) at 24 weeks for the *virD4* mutants; $p<0.001$ for each). Antibody titres of gerbils infected with the *cagG* mutants were very low (maximum 3.5), and even seroconversion occurred.

Histopathological findings

Histopathological changes at 4, 12, and 24 weeks after inoculation of Mongolian gerbils with *H pylori* and in controls are shown in fig 2. Inflammatory cell infiltration in the lamina propria was negligible in controls. At four weeks after inoculation, gerbils infected with the wild-type strains showed chronic active gastritis in the antrum, with marked mucosal infiltration by neutrophilic polymorphonuclear cells (PMN) (infiltration score 1.0 (0.3)) and by mononuclear cells (MNC) (1.9 (0.3)) (figs 3, 4). At 12 weeks, with the wild-type strains, dense PMN infiltration was seen throughout the mucosa with a dense MNC infiltration in the lamina propria and submucosa in the antrum, with the normal mucosal architecture being almost completely replaced with hyperplastic epithelium (PMN 2.5 (0.2) and 0.7 (0.2); MNC 2.8 (0.1) and 1.0 (0.2) for the antrum and corpus, respectively). At 24 weeks with the wild-type strains, numerous irregularly branched dilated mucous glands were seen in the lower portion of the proper muscle layer and the PMN and MNC infiltration scores reached their maximal levels (PMN 3.0 and 1.0 (0.2); MNC 3.0 and 1.1 (0.1) for the antrum and corpus, respectively).

In contrast, gerbils infected with the *cagG* mutants showed almost no inflammation at any time after inoculation (figs 3, 4). MNC and PMC infiltration scores in gerbils infected with the *cagG* mutants were significantly lower than those with the wild-type strain throughout the observation periods.

Gerbils infected with the *virD4* mutants showed mild cellular inflammation four and 12 weeks after inoculation (MNC and PMC infiltration scores less than 0.5). MNC and PMC infiltration scores in gerbils infected with the *virD4* mutants were significantly lower than those with the wild-type strains throughout the observation periods. Interestingly, however, at 24 weeks after inoculation, gerbils infected with the *virD4* mutants showed chronic active gastritis with marked mucosal infiltration in the antrum (MNC 1.8 (0.3) and PMN 1.3 (0.3)) whereas mucosal infiltration in the corpus remained very mild (figs 3, 4). The amount of cellular infiltration in the antrum increased in gerbils infected with the *virD4* mutants at 24 weeks

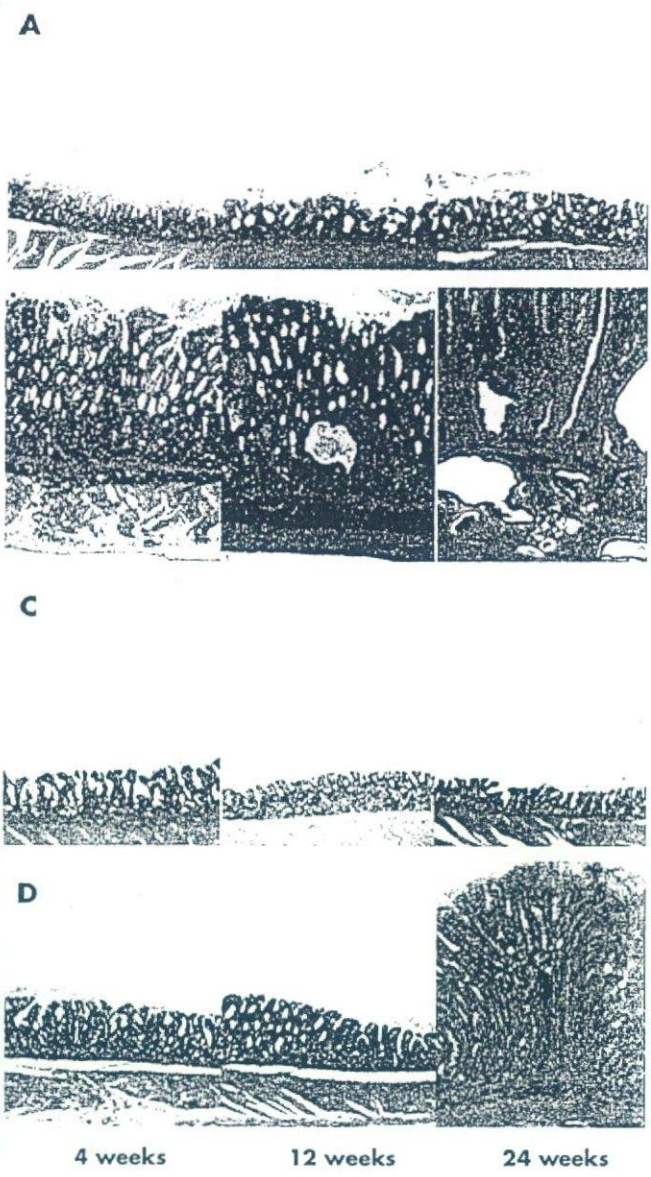

Figure 2 Histology of the gastric pyloric mucosa of (A) control, (B) wild-type *Helicobacter pylori* strain TN2GF4, (C) its isogenic *cagG* knockout mutant, or (D) *virD4* knockout mutant. Haematoxylin and eosin stain, original magnification ×200. (A) In controls, inflammatory cell infiltration in the lamina propria was negligible throughout the experimental periods. (B) In gerbils infected with the wild-type strain, pyloric mucosa showed marked infiltration by neutrophilic polymorphonuclear cells and mononuclear cells at four weeks after inoculation and the inflammatory response increased with the duration of infection. The pyloric mucosa became thickened from four weeks after inoculation, and irregularly branched and dilated mucous glands appeared at 24 weeks after inoculation. (C) In gastric mucosa infected with the *cagG* knockout mutants, inflammatory cell infiltration in the lamina propria was negligible throughout the experimental periods. (D) Pyloric mucosa of gerbils infected with the *virD4* knockout mutants showed mild inflammatory inflammation at four and 12 weeks after inoculation. At 24 weeks after inoculation, pyloric mucosa showed increased degrees of inflammatory cell infiltration and became thickened.

compared with 12 weeks, and the pyloric mucosa appeared expanded similar to that observed with the wild-type strains. The grade of mucosal inflammation observed in gerbils infected with the *virD4* mutants at 24 weeks was similar to those with the wild-type strains at four weeks.

H pylori density score, as evaluated by histology in the antrum of gerbils infected with the *virD4* mutants, was significantly greater than that in animals infected with the wild-type strains at 24 weeks (fig 5) ($p<0.01$). Importantly,

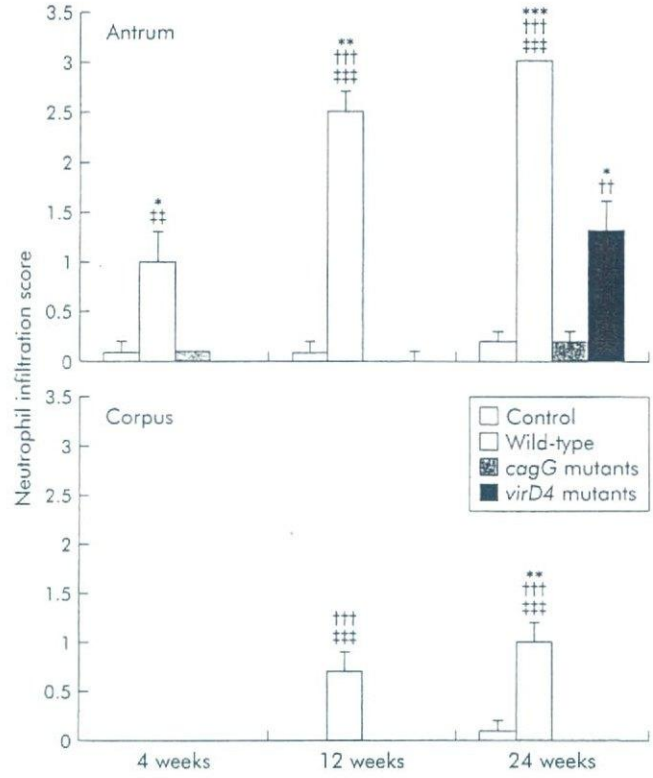

Figure 3 Neutrophil infiltration scores at 4, 12, and 24 weeks after inoculating with *Helicobacter pylori* or without *H pylori* (control). Mean (SEM) values are presented. *p<0.05, **p<0.01, ***p<0.001 compared with control; ††p<0.01, †††p<0.001 compared with the *cagG* knockout mutants; ‡‡p<0.01, ‡‡‡p<0.001 compared with the *virD4* knockout mutants.

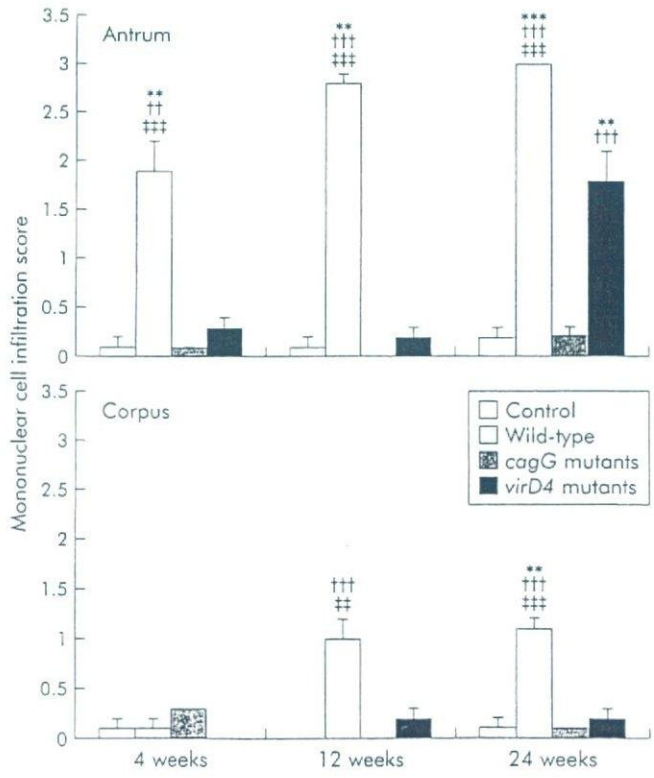

Figure 4 Mononuclear cell infiltration scores at 4, 12, and 24 weeks after inoculating with *Helicobacter pylori* or without *H pylori* (control). Mean (SEM) values are presented. **p<0.01, ***p<0.001 compared with control; ††p<0.01, †††p<0.001 compared with the *cagG* knockout mutants; ‡‡p<0.01, ‡‡‡p<0.001 compared with the *virD4* knockout mutants.

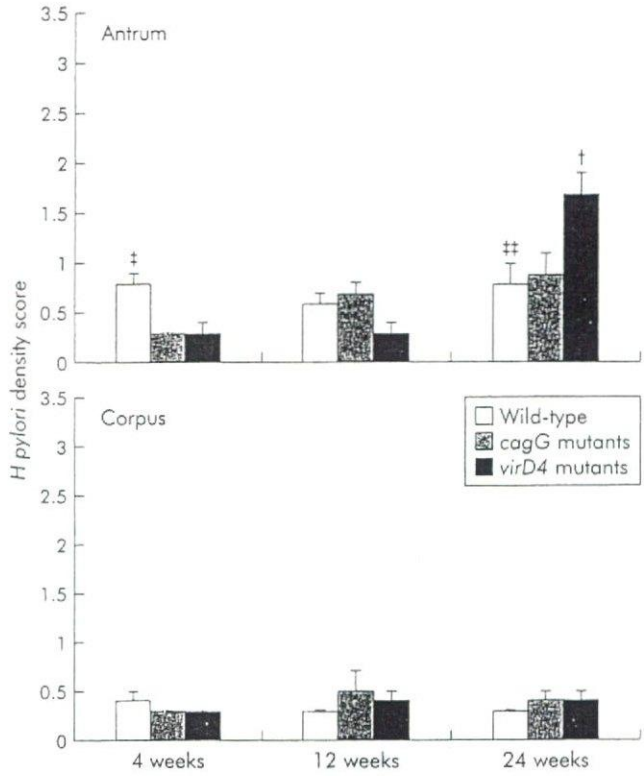

Figure 5 Scores for *Helicobacter pylori* density evaluated by histology at 4, 12, and 24 weeks after inoculation with *H pylori*. Mean (SEM) values are presented. †p<0.05 compared with the *cagG* knockout mutants, ‡p<0.05, ‡‡p<0.01 compared with the *virD4* knockout mutants.

gerbils infected with the *cagG* mutants showed no inflammation at any time after inoculation. *H pylori* density score was mostly equivalent to the wild-type strains or *virD4* mutants (fig 5).

BrdU labelling indices

Detectable BrdU labelling indices were not observed in control gerbils without *H pylori* infection. BrdU labelling indices in the antrum were independent of the duration of *H pylori* infection both in gerbils infected with the wild-type strains (mean 26.3 (3.1) to 34.6 (3.3)) and the *cagG* mutants (mean 3.2 (0.5) to 11.3 (7.3)) (fig 6). In contrast, BrdU labelling indices were significantly increased in the *virD4* mutants at 24 weeks after inoculation (29.3 (3.9) at 24 weeks compared with 6.1 (0.8) at four weeks and 3.8 (0.5) at 12 weeks) (p<0.001 for each). Overall, BrdU labelling indices were higher in gerbils infected with the wild-type strains compared with those with the *cagG* mutants or the *virD4* mutants at four or 12 weeks. Indices were also significantly higher in gerbils infected with the wild-type strains compared with those with the *cagG* mutants at 24 weeks (p<0.001) whereas the indices were similar among gerbils infected with the wild-type strains and the *virD4* mutants.

Mucosal IL-1β mRNA levels

In the control group, mucosal IL-1β mRNA levels were very low throughout the observation periods (10 000× mean (SEM); IL-1β/GAPDH 1.8 (0.4) to 6.6 (0.8)) (fig 7). At four weeks after inoculation, mucosal IL-1β mRNA levels were significantly greater in gerbils infected with the wild-type strains compared with the *virD4* or *cagG* mutants. Mucosal IL-1β mRNA levels at 12 weeks with the wild-type strains were also significantly higher than those with the *virD4* or

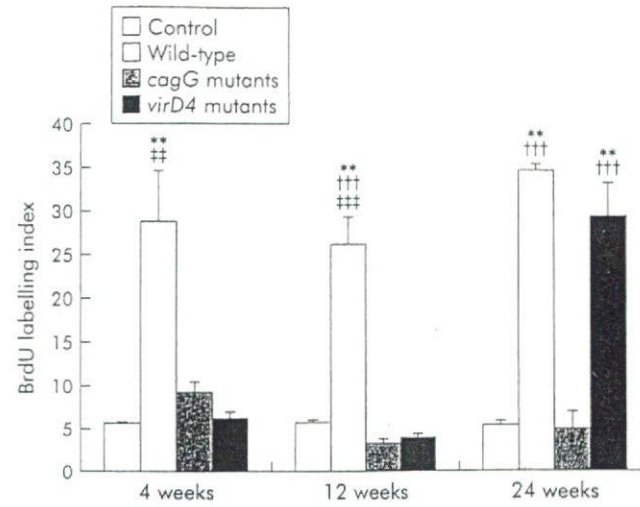

Figure 6 5′-Bromo-2′deoxyuridine (BrdU) labelling indices in the pyloric mucosa. Mean (SEM) values are presented. **p<0.01 compared with control; †††p<0.001 compared with the *cagG* knockout mutants; ‡‡p<0.01, ‡‡‡p<0.001 compared with the *virD4* knockout mutants.

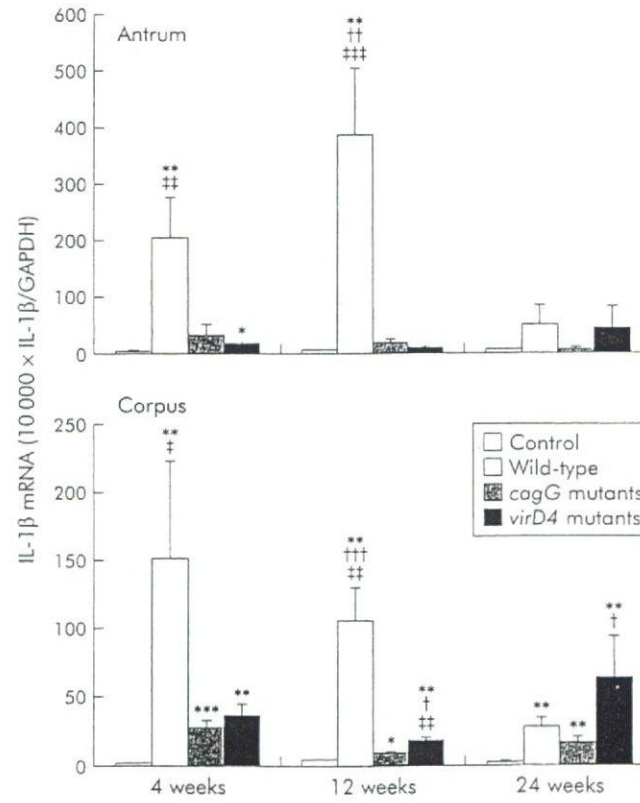

Figure 7 Mucosal interleukin (IL)-1β mRNA levels in gerbils at 4, 12, and 24 weeks after inoculating with *Helicobacter pylori* or without *H pylori* (control) in the pyloric mucosa (antrum) and fundic mucosa (corpus). Mean (SEM) values are presented. *p<0.05, **p<0.01, ***p<0.001 compared with control; †p<0.05, ††p<0.01, †††p<0.001 compared with the *cagG* knockout mutants; ‡‡p<0.01, ‡‡‡p<0.001 compared with the *virD4* knockout mutants.

cagG mutants. At 24 weeks after inoculation, IL-1β levels decreased in gerbils infected with the wild-type strains.

Mucosal IL-1β levels were very low in gerbils infected with the *virD4* mutants throughout the first 12 weeks; however, these levels tended to increase at 24 weeks (45.6 (36.0) for the antrum and 63.0 (30.6) for the corpus). In contrast, IL-1β

www.gutjnl.com

levels were very low in gerbils infected with the *cagG* mutants throughout the observation periods (fig 7).

DISCUSSION

We used the Mongolian gerbil model to examine the effect of two previously unstudied genes in the *cag* PAI (*virD4* and *cagG*) on gastric inflammation in vivo. Wild-type *H pylori* caused typical severe gastritis in gerbils whereas the *virD4* mutants caused very low levels of gastric inflammation, mucosal proliferative activity, and mucosal IL-1β levels throughout the first 12 weeks. *H pylori* density was similar with the different inocula, confirming that the differences were not due to bacterial load. At 24 weeks, the degree of gastric inflammation and proliferative activity in gerbils infected with the *virD4* mutants increased, reaching levels comparative with those seen at four weeks with the wild-type strains. *H pylori* density in the antrum at 24 weeks in gerbils infected with the *virD4* mutants was significantly higher than that with wild-type *H pylori* ($p = 0.03$). Lack of acute inflammation might help growth of the *virD4* mutants; however, it remains unclear whether it is sufficient to explain the results.

Mucosal IL-1β levels at 24 weeks were similar for *virD4* mutants and wild-type infections. IL-1β levels with the wild-type strains were maximal at four weeks in the corpus and at 12 weeks in the antrum. In gerbils and in mice, IL-1β mRNA levels do not mirror chronic mucosal inflammation.[27 28] In contrast, in humans, IL-1β levels are consistently elevated in *H pylori* infected gastric mucosa.[23] IL-1β mRNA levels in the corpus were very low in the chronic phase of the infection, suggesting that induction of acute inflammation rather than inhibition of gastric acid secretion[29 30] is the main role of IL-1β in gerbils. Probably the most important proinflammatory cytokine in the gastric mucosa is IL-8. Gerbils do not encode an IL-8 gene, as cross species RT-PCR techniques failed to identify an IL-8 gene (unpublished observation). We selected IL-1β based on the fact that in humans, mucosal IL-8 levels were closely correlated with mucosal IL-1β levels.[23 31] Future studies will examine cytokine expression using IL-8 families such as KC which behave like IL-8 in mice.

With the wild-type strains, the degree of gastric inflammation reached maximal levels at 12–26 weeks and proliferative activity at four weeks.[25 32 33] Loss of the *virD4* gene temporally retarded but did not abrogate *H pylori* induced gastric inflammation, and proliferative activity with the *virD4* mutants was similar to that with the wild-type strains at 24 weeks. We did not examine animals beyond 24 weeks and can only speculate regarding later time points.

The *virB4* (*cagE*) knockout mutants produce mild gastritis and not gastric ulcers.[13–15] VirB4 is a major component of the type IV secretion system such that loss of the *cagE* gene results in loss of CagA translocation/phosphorylation as well as loss of host cytoskeletal rearrangement and IL-8 induction.[3 12 17] Although the *virD4* mutants also lose the ability to translocate CagA into host cells, *cagA* mutants can produce inflammation[16] consistent with in vitro studies showing that CagA is not responsible for IL-8 induction. Lack of inflammation with the *virD4* mutants in the first 12 weeks suggests the absence of as yet unidentified factors that translocate into epithelial cells using the type IV secretory pathway or interact with the type IV secretion system. Several factors other than the *cag* PAI, in particular OipA as one of the outer membrane proteins, are related to induction of mucosal IL-8 and gastric inflammation.[22 34 35] In addition, *cag* PAI status is closely related to OipA status (for example, if the strains possess the *cag* PAI, strains almost always possess functional OipA).[34] However, possible interactions between OipA and *cag* PAI were not examined in these experiments.

The *cagG* mutants did not produce an inflammatory response or increase proliferative activity, most likely related to their poor ability to colonise gerbil gastric mucosa. The *cagG* gene is not a *vir* homologue gene and has a weak homology to the flagellar motor switch protein gene or toxin coregulated pilus biosynthesis protein gene.[3 20] The current consensus is that loss of the *cagG* gene also results in loss of CagA translocation/phosphorylation.[3 12] Recent reports suggest that isolates lacking *cagG* genes have decreased adherence to epithelial cell lines.[19] An in vivo study has shown no relationship between *cagG* and clinical outcome[36]; the population studied (Chinese) were predominantly infected with *cag* PAI positive strains such that the effect of the *cagG* gene could not be examined. Most reports, including our present study, suggest that loss of the *cagG* gene results in almost complete elimination of *H pylori* induced IL-8

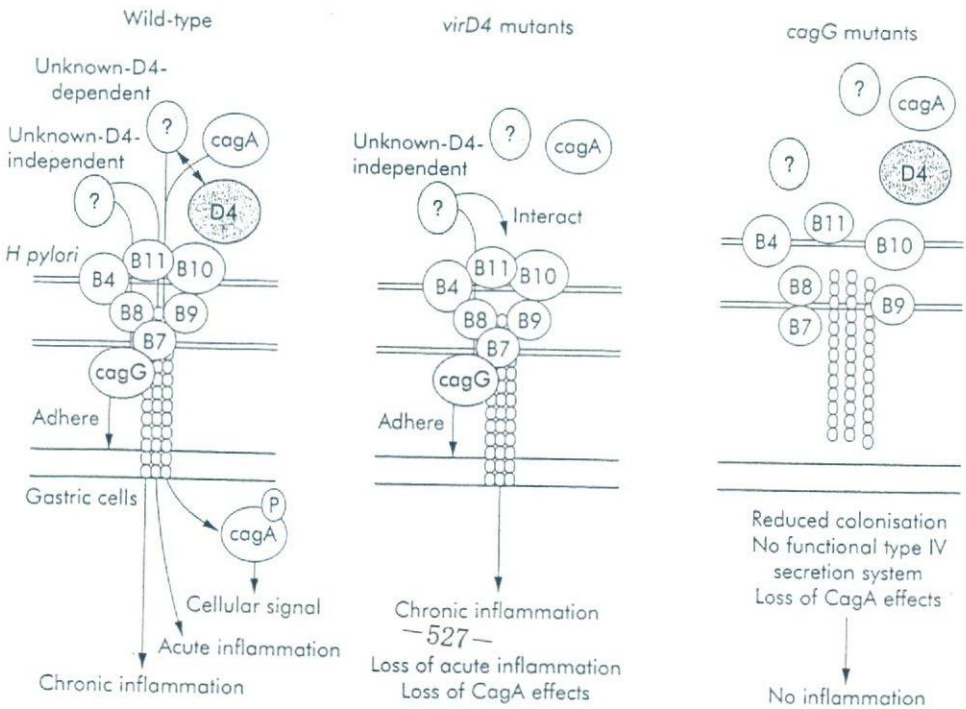

Figure 8 Hypothetical model for induction of host responses by *Helicobacter pylori*.

induction.[3 37] However, a recent report suggested that precise deletion of the *cagG* gene resulted in no reduction in IL-8 induction.[12] Gerbils infected with *cagG* mutants showed no inflammation although the *H pylori* density score was generally equivalent to wild-type strains or *virD4* mutants (fig 5). From these data it is not possible to define whether or not the lack of inflammation with *cagG* mutants is related to reduced colonisation, loss of the type IV secretion system, or both. Complementation experiments will be needed to resolve this issue.

Our current hypothetical model is presented in fig 8. VirD4 is thought to act as an adapter protein for the transfer of CagA protein and possibly other unknown proteins (D4 dependent) into the transfer channel formed by other Vir proteins in the *cag* PAI. We also hypothesise the presence of unknown proteins independent of VirD4. As *virD4* mutants are unable to translocate CagA as well as any D4 dependent factors, loss of CagA effects and loss of D4 dependent factors occurs. However, it is possible that D4 independent factors may be translocated into cells or interact with the type IV secretion system, inducing chronic inflammation. *cagG* mutants have decreased adherence to epithelial cells and reduced ability to colonise gerbils. In addition, they are unable to translocate CagA and any D4 dependent or independent factors due to loss of functional transporter system such that inflammation would not be expected.

ACKNOWLEDGMENTS

This study was supported by Grants-in-Aid for Scientific Research C-15590482 (to HO) from the Ministry of Education, Culture, Sports, Science, and Technology of Japan, by a grant from the Hokuto Foundation for Bioscience (to HO), and by National Institutes of Health grants R01 DK62813 (to YY) Drs Graham and Yamaoka are supported in part by the Office of Research and Development Medical Research Service Department of Veterans Affairs. We thank M Nakao, Takeda Chemical Industries, Ltd, Osaka, Japan, for providing the *H pylori* isolate TN2GF4 and DE Taylor, University of Alberta, Edmonton, Canada, for providing a chloramphenicol resistance gene cassette.

Authors' affiliations

H Saito, S Ishizone, F Maruta, A Sugiyama, S Miyagawa, Department of Surgery, Shinshu University School of Medicine, Matsumoto, Nagano, Japan
Y Yamaoka, D Y Graham, Department of Medicine, Michael E DeBakey Veterans Affairs Medical Center and Baylor College of Medicine, Houston, Texas, USA
K Yamauchi, Department of Laboratory Medicine, School of Health Science, Shinshu University Hospital, Matsumoto, Nagano, Japan
H Ota, Department of Biomedical Laboratory Sciences, School of Health Science, Shinshu University School of Medicine, Matsumoto, Nagano, Japan

Conflict of interest: None declared.

REFERENCES

1 **Graham DY**. Helicobacter pylori infection in the pathogenesis of duodenal ulcer and gastric cancer: a model. *Gastroenterology* 1997;**113**:1983–91.
2 **Graham DY**, Yamaoka Y. H. pylori and cagA: relationships with gastric cancer, duodenal ulcer, and reflux esophagitis and its complications, *Helicobacter* 1998;**3**:145–51.
3 **Censini S**, Lange C, Xiang Z, *et al.* cag, a pathogenicity island of Helicobacter pylori, encodes type I-specific and disease-associated virulence factors. *Proc Natl Acad Sci U S A* 1996;**93**:14648–53.
4 **Blaser MJ**, Perez-Perez GI, Kleanthous H, *et al.* Infection with Helicobacter pylori strains possessing cagA is associated with an increased risk of developing adenocarcinoma of the stomach. *Cancer Res* 1995;**55**:2111–15.
5 **Segal ED**, Cha J, Lo J, *et al.* Altered states: involvement of phosphorylated CagA in the induction of host cellular growth changes by Helicobacter pylori. *Proc Natl Acad Sci U S A* 1999;**96**:14559–64.
6 **Stein M**, Rappuoli R, Covacci A. Tyrosine phosphorylation of the Helicobacter pylori CagA antigen after cag-driven host cell translocation. *Proc Natl Acad Sci U S A* 2000;**97**:1263–8.
7 **Asahi M**, Azuma T, Ito S, *et al.* Helicobacter pylori CagA protein can be tyrosine phosphorylated in gastric epithelial cells. *J Exp Med* 2000;**191**:593–602.
8 **Backert S**, Ziska E, Brinkmann V, *et al.* Translocation of the Helicobacter pylori CagA protein in gastric epithelial cells by a type IV secretion apparatus. *Cell Microbiol* 2000;**2**:155–64.
9 **Odenbreit S**, Puls J, Sedlmaier B, *et al.* Translocation of Helicobacter pylori CagA into gastric epithelial cells by type IV secretion. *Science* 2000;**287**:1497–500.
10 **Selbach M**, Moese S, Hauck CR, *et al.* Src is the kinase of the Helicobacter pylori CagA protein in vitro and in vivo. *J Biol Chem* 2002;**277**:6775–8.
11 **Covacci A**, Telford JL, Del Giudice G, *et al.* Helicobacter pylori virulence and genetic geography. *Science* 1999;**284**:1328–33.
12 **Fischer W**, Puls J, Buhrdorf R, *et al.* Systematic mutagenesis of the Helicobacter pylori cag pathogenicity island: essential genes for CagA translocation in host cells and induction of interleukin-8. *Mol Microbiol* 2001;**42**:1337–48.
13 **Sakai T**, Fukui H, Franceschi F, *et al.* Cyclooxygenase expression during Helicobacter pylori infection in Mongolian gerbils. *Dig Dis Sci* 2003;**48**:2139–46.
14 **Ogura K**, Maeda S, Nakao M, *et al.* Virulence factors of Helicobacter pylori responsible for gastric diseases in Mongolian gerbil. *J Exp Med* 2000;**192**:1601–10.
15 **Israel DA**, Salama N, Arnold CN, *et al.* Helicobacter pylori strain-specific differences in genetic content, identified by microarray, influence host inflammatory responses. *J Clin Invest* 2001;**107**:611–20.
16 **Wirth HP**, Beins MH, Yang M, *et al.* Experimental infection of Mongolian gerbils with wild-type and mutant Helicobacter pylori strains. *Infect Immun* 1998;**66**:4856–66.
17 **Selbach M**, Moese S, Meyer TF, *et al.* Functional analysis of the Helicobacter pylori cag pathogenicity island reveals both VirD4-CagA-dependent and VirD4-CagA-independent mechanisms. *Infect Immun* 2002;**70**:665–71.
18 **Crabtree JE**, Kersulyte D, Li SD, *et al.* Modulation of Helicobacter pylori induced interleukin-8 synthesis in gastric epithelial cells mediated by *cag* PAI encoded VirD4 homologue. *J Clin Pathol* 1999;**52**:653–7.
19 **Mizushima T**, Sugiyama T, Kobayashi T, *et al.* Decreased adherence of cagG-deleted Helicobacter pylori to gastric epithelial cells in Japanese clinical isolates. *Helicobacter* 2002;**7**:22–9.
20 **Tomb JF**, White O, Kerlavage AR, *et al.* The complete genome sequence of the gastric pathogen Helicobacter pylori. *Nature* 1997;**388**:539–47.
21 **Christie PJ**, Vogel JP. Bacterial type IV secretion: conjugation systems adapted to deliver effector molecules to host cells. *Trends Microbiol* 2000;**8**:354–60.
22 **Yamaoka Y**, Kwon DH, Graham DY. A M(r) 34,000 proinflammatory outer membrane protein (oipA) of Helicobacter pylori. *Proc Natl Acad Sci U S A* 2000;**97**:7533–8.
23 **Yamaoka Y**, Kita M, Kodama T, *et al.* Induction of various cytokines and development of severe mucosal inflammation by cagA gene positive Helicobacter pylori strains. *Gut* 1997;**41**:442–51.
24 **Dixon MF**, Genta RM, Yardley JH, *et al.* Classification and grading of gastritis: the updated Sydney system. *Am J Surg Pathol* 1996;**20**:1161–81.
25 **Ikeno T**, Ota H, Sugiyama A, *et al.* Helicobacter pylori-induced chronic active gastritis, intestinal metaplasia, and gastric ulcer in Mongolian gerbils. *Am J Pathol* 1999;**154**:951–60.
26 **Kumagai T**, Yan J, Graham DY, *et al.* Serum immunoglobulin G immune response to Helicobacter pylori antigens in Mongolian gerbils. *J Clin Microbiol* 2001;**39**:1283–8.
27 **Takashima M**, Furuta T, Hanai H, *et al.* Effects of Helicobacter pylori infection on gastric acid secretion and serum gastrin levels in Mongolian gerbils. *Gut* 2001;**48**:765–73.
28 **Fox JG**, Wang TC, Rogers AB, *et al.* Host and microbial constituents influence Helicobacter pylori-induced cancer in a murine model of hypergastrinemia. *Gastroenterology* 2003;**124**:1879–90.
29 **Uehara A**, Okumura T, Sekiya C, *et al.* Interleukin-1 inhibits the secretion of gastric acid in rats: possible involvement of prostaglandin. *Biochem Biophys Res Commun* 1989;**162**:1578–84.
30 **Wallace JL**, Cucala M, Mugridge K, *et al.* Secretagogue-specific effects of interleukin-1 on gastric acid secretion. *Am J Physiol* 1991;**261**:G559–64.
31 **Yamaoka Y**, Kodama T, Kita M, *et al.* Relation between clinical presentation, Helicobacter pylori density, interleukin-1β and -8 production and cagA status. *Gut* 1999;**45**:804–11.
32 **Watanabe T**, Tada M, Nagai H, *et al.* Helicobacter pylori infection induces gastric cancer in Mongolian gerbils. *Gastroenterology* 1998;**115**:642–8.
33 **Sawada Y**, Kuroda Y, Sashio H, *et al.* Pathological changes in glandular stomach of Helicobacter pylori-infected Mongolian gerbil model. *J Gastroenterol* 1998;**33**(suppl 10):22–5.
34 **Yamaoka Y**, Kikuchi S, El-Zimaity HMT, *et al.* Importance of Helicobacter pylori OipA in clinical presentation, gastric inflammation, and mucosal interleukin-8 production. *Gastroenterology* 2002;**123**:414–24.
35 **Yamaoka Y**, Kudo T, Lu H, *et al.* Role of interferon stimulated responsive element-like element in interleukin-8 promoter in Helicobacter pylori infection. *Gastroenterology* 2004;**126**:1030–43.
36 **Xu C**, Li ZS, Tu ZX, *et al.* Distribution of cagG gene in Helicobacter pylori isolates from Chinese patients with different gastroduodenal diseases and its clinical and pathological significance. *World J Gastroenterol* 2003;**9**:2258–60.
37 **Hsu PI**, Hwang IR, Cittelly D, *et al.* Clinical presentation in relation to diversity within the Helicobacter pylori cag pathogenicity island. *Am J Gastroenterol* 2002;**97**:2231–8.

Transplant International ISSN 0934-0874

ORIGINAL ARTICLE

MCI-186 (edaravone), a free radical scavenger, attenuates hepatic warm ischemia–reperfusion injury in rats

Fumitaka Suzuki,[1,2] Yasuhiko Hashikura,[2] Hirohiko Ise,[1] Akiko Ishida,[3] Jun Nakayama,[3] Masafumi Takahashi,[1] Shin-ichi Miyagawa[2] and Uichi Ikeda[1]

1 Department of Organ Regeneration, Shinshu University Graduate School of Medicine, Asahi, Matsumoto, Japan
2 First Department of Surgery, Shinshu University School of Medicine, Asahi, Matsumoto, Japan
3 Department of Pathology, Shinshu University School of Medicine, Asahi, Matsumoto, Japan

Keywords
chemokine, Kupffer cell, lipid peroxidation, macrophage, neutrophil.

Correspondence
Yasuhiko Hashikura MD, First Department of Surgery, Shinshu University School of Medicine, 3-1-1 Asahi, Matsumoto 390-8621, Japan. Tel.: +81-263-37-2654; fax: +81-263-35-1282; e-mail: yh@hsp.md.shinshu-u.ac.jp

Received: 17 November 2004
Revision requested: 7 December 2004
Accepted: 20 December 2004

doi:10.1111/j.1432-2277.2005.00094.x

Summary

Hepatic warm ischemia–reperfusion injury (IRI) during hepatectomy and liver transplantation is a major cause of liver dysfunction in which the pathologic role of free radicals is a major concern. To assess the effect of MCI-186 (edaravone) on hepatic IRI, male Wistar rats were subjected to partial hepatic ischemia for 60 min after pretreatment with vehicle (group C) or MCI-186 (group M), or after both MCI-186 pretreatment and additional administration of MCI-186 12 h after reperfusion (group MX). Groups M and MX showed significantly lower levels of serum alanine aminotransferase and hepatic lipid peroxidation than group C, and also significantly lower expression levels of mRNA for cytokines, chemokines and intercellular adhesion molecule-1. There were fewer tissue monocytes and neutrophils in groups M and MX than in group C. These effects were more marked in group MX than in group M. Our findings suggest that treatment with MCI-186 attenuates hepatic IRI in this rat *in vivo* model.

Introduction

Warm ischemia–reperfusion injury (IRI) during hepatic resection and liver transplantation may lead to local and systemic organ dysfunction. The local hepatic injury comprises two phases, the acute (early) phase and the subacute (late) phase [1–9]. During the acute phase, Kupffer cells are activated and release oxygen-derived free radicals (ODFRs) and proinflammatory cytokines such as tumor necrosis factor (TNF)-α, interleukin (IL)-1, IL-6 and IL-8. The subacute phase is mediated by infiltrating neutrophils that are primed and activated during the acute phase [1–9]. Chemokines released by Kupffer cells, including CXC chemokines and CC chemokines, may also play important roles in hepatic IRI. CXC chemokines induce neutrophil activation and CC chemokines activate macrophages and T cells and upregulate cell adhesion molecules [10–13]. While recent studies have shown that not only macrophages (Kupffer cells) and neutrophils but also T cells play significant roles in hepatic IRI [3,5,6,14,15], the significance of free radicals in the pathology of the acute and subacute phases of hepatic IRI is thought to be crucial.

MCI-186 [edaravone (3-methyl-1-phenyl-2-pyrazolin-5-one); Mitsubishi Pharma Co., Osaka, Japan] is a free radical scavenger. This reagent has already been applied clinically for the prevention of brain edema in patients with acute cerebral infarction through inhibition of the lipoxygenase pathway in the arachidonic acid cascade and has shown positive results [16–19]. Several reports have described the effects of MCI-186 on hepatic IRI. In *ex vivo* hepatic IRI experiments [20,21], perfusion with Krebs–Henseleit solution cannot reproduce the effects of circulating macrophages and neutrophils, which play major roles in hepatic IRI. In *in vivo* experiments, the efficacy of MCI-186 in attenuating hepatic warm IRI has been evaluated in terms of aspartate aminotransferase, phosphatidylcholine hydroperoxide, adenosine triphosphate [22], and mitochondrial function [23]. However,

the effects of MCI-186 on monocytes, neutrophils and their associated cytokines have not been evaluated.

In the present study, we evaluated the potential of MCI-186 to attenuate hepatic warm IRI in a partial-IRI rat model *in vivo*. We focused on the changes in lipoxygenase activation, monocyte activation, chemokine expression, neutrophil infiltration and hepatic dysfunction resulting from administration of MCI-186.

Materials and methods

Experimental animals and reagents

Male Wistar rats (Clea Japan Inc., Tokyo, Japan) weighing 200–250 g were used. All animals were maintained under standard conditions and fed rodent chow and water *ad libitum*. Twelve hours before surgery, the animals were fasted, but allowed access to water. All experimental procedures were reviewed and approved by the Institutional Animal Care and Use Committee of Shinshu University.

The following monoclonal antibodies were used as primary antibodies for immunohistochemistry: HNEJ-2 (Nikken Seil Co., Shizuoka, Japan) specific for 4-hydroxy-2-nonenal (4-HNE) modified protein, ED-1 (Serotec, Oxford, UK) specific for rat CD163 expressed on free and fixed macrophages, ED-2 (Serotec) specific for rat CD68 expressed on Kupffer cells and on residential macrophages, and HIS48 (BD Biosciences, Palo Alto, CA, USA) specific for rat neutrophils.

Hepatic IRI model

All surgical procedures were carried out according to the protocol described elsewhere [24]. Rats were anesthetized with sodium pentobarbital 50 mg/kg, intraperitoneally (Dainippon Pharmaceutical Co. Ltd, Osaka, Japan). After laparotomy, a microvascular clip (BEAR Medic Co., Chiba, Japan) was used to interrupt the arterial and portal venous supply to the median and left lateral lobes of the liver. This resulted in ischemia of approximately 70% of the whole liver while avoiding portal venous congestion. After 60 min of partial hepatic ischemia, the clamp was removed for reperfusion. The abdomen was closed and 1 ml of saline was administered intravenously. The rats were killed 1, 3, 6 and 24 h after reperfusion, and blood and tissue samples were harvested for analysis.

Experimental protocol

The rats were divided into three groups(Fig. 1). Group S was a sham operation group. Group C comprised IRI model rats, administered saline 5 min before reperfusion. Group M comprised IRI model rats, administered MCI-186 (3 mg/kg) 5 min before reperfusion. Saline and MCI-186 were injected intravenously. The dose and timing of saline and MCI-186 administration were based on previous reports [25–27].

Each group was divided into four subgroups according to the time (h) from reperfusion to killing [groups S-1, S-3, S-6, S-24 ($n = 5$, respectively), C-1 ($n = 6$), C-3 ($n = 5$), C-6 ($n = 7$), C-24 ($n = 7$), M-1 ($n = 6$), M-3 ($n = 5$), M-6 ($n = 7$) and M-24 ($n = 5$)]. For groups S-24, C-24 and M-24, additional administration of saline was performed 12 h after reperfusion.

In addition, considering the short half-life of MCI-186 as well as the acute and subacute mechanisms underlying IRI, a fourth group was additionally administered MCI-186 12 h after reperfusion instead of saline, followed by killing 24 h after reperfusion [group MX-24 ($n = 7$)]. This protocol was used to evaluate the role of MCI-186 in the subacute phase of IRI.

Peripheral blood and tissue samples

Blood samples were obtained via the abdominal aorta. The blood was centrifuged (2500 *g*, 10 min) at room temperature and the plasma was collected and stored at −20 °C until use. Portions of the ischemic and nonischemic lobes were fixed in 10% buffered formalin and embedded in paraffin. Other portions were snap-frozen in

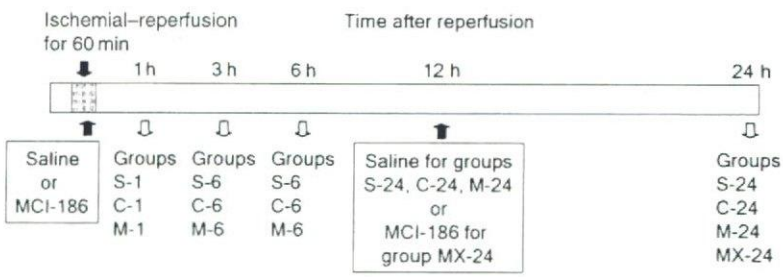

Figure 1 Experimental protocols for rat hepatic ischemia–reperfusion injury models.

liquid nitrogen to extract mRNA and embedded in optimal cutting temperature (OCT) compound (Sakura Finetechnical Co., Tokyo, Japan) for immunohistochemistry, and stored at −80 °C until used.

Measurement of serum aminotransferase

To evaluate hepatic injury, we measured serum alanine aminotransferase (ALT) levels at the time of killing in each group using an AU5232 autoanalyzer (Olympus, Tokyo, Japan), as described previously [24].

Histologic examination

Samples were fixed with 10% buffered formaldehyde and embedded in paraffin. Sections at 3-μm intervals were prepared and stained with hematoxylin and eosin for histologic examination. A blinded analysis was performed by two pathologists to determine the degree of lesions observed ($n = 5$, independent animals in each group). The degrees of sinusoidal congestion, cytoplasmic vacuolization and necrosis of parenchymal cells were evaluated semiquantitatively according to the criteria described in a previous study [28].

Immunohistochemistry

Immunohistochemical detection of lipid peroxidation and inflammatory cell recruitment was carried out. For detection of 4-HNE and macrophages, 10% buffered formaldehyde-fixed and paraffin-embedded tissue samples were cut into 3-μm-thick sections. Antigen retrieval was performed by 25 min of microwave irradiation in 1.0 mM EDTA-Na_2 for 4-HNE, and by 6 min of proteinase K digestion (0.4 mg/ml) for ED-2. No retrieval procedure was performed for ED-1. After antigen retrieval, the sections were incubated with primary antibodies at 4 °C overnight for 4-HNE and at room temperature for 60 min for ED-1 and ED-2. The dilutions of the primary antibodies were 1:80 for 4-HNE, 1:200 for ED-1 and 1:100 for ED-2. Goat anti-mouse immunoglobulin conjugated with peroxidase-labeled dextran polymer (Envision™+ system; Dako, Carpinteria, CA, USA) was used as the secondary antibody.

For detection of neutrophils, we used frozen sections. Samples embedded in OCT compound were cut into 5-μm-thick sections, placed on adhesive-coated slides (Matsunami Glass, Osaka, Japan), and then air-dried. After blocking with 1% normal goat serum in tris-buffered saline, these tissue specimens were incubated at room temperature for 60 min with a primary monoclonal antibody, HIS48. After washing with phosphate-buffered saline, the specimens were incubated using the Envision™+ system.

In a control experiment, the primary antibody was omitted from the staining procedure, and no specific staining was found. Counterstaining was carried out with hematoxylin.

Analysis of mRNA by reverse transcription-polymerase chain reaction (RT-PCR)

Total RNA was extracted from tissue with ISOGEN (Nippon Gene Co. Ltd, Tokyo, Japan). cDNA was reverse-transcribed from 2 μg of total RNA using an Omniscript™ Reverse Transcriptase kit (Qiagen GmbH, Hilden, Germany). The cDNA was amplified by RT-PCR using a *Taq* polymerase core kit (Qiagen GmbH). We prepared primer sets for RT-PCR as shown in Table 1, and the final reaction volume was 25 μl. The samples were loaded into a thermal cycler after determining the optimal number of cycles as follows: 30 cycles of denaturing at 94 °C for 1 min, annealing at 55 °C for 1 min, and extension at 72 °C for 2 min for TNF-α and IL-1β; 30 cycles at 94 °C for 30 s, 58 °C for 1 min, and 72 °C for 1 min for cytokine-induced neutrophil chemoattractant (CINC)-2 and macrophage inflammatory protein (MIP)-2; 25 cycles at 94 °C for 30 s, 60 °C for 1 min, and 72 °C

Table 1. Polymerase chain reaction primer sets for cytokines, chemokines, and adhesion molecule.

	Sense (5′ → 3′)	Anti-sense (5′ → 3′)
β-actin	CGG CAT TGT AAC CAA CAG G	CAT TGC CGA TAG TGA TGA CC
TNF-α	TAC TGA ACT TCG GGG TGA TTG GTC C	CAG CCT TGT CCC TTG AAG AGA A
IL-1β	GCT ACC TAT GTC TTG CCC GT	GAC CAT TGC TGT TTC CTA GG
CINC-2	GCT ACC TAT GTC TTG CCC GT	TGA CCA TCC TTG GAG AGT GGC
MIP-2	AGC TCC TCA ATG CTG TAC TGG	TCT ATC ACA GTG TGG AGG TGG
MCP-1	CTC TTC CTC CAC CAC TAT GC	CTC TGT CAT ACT GGT CAC TTC
MIP-1α	GAA GGA AAG TCT TCT CAG CG	AGA CAT TCA GTT CCA GC
MIP-1β	ATG AAG CTC TGC GTG TCT GC	AGT TCC GAT GAA TCT TCC GG
ICAM-1	GAT GCT GAC CCT CCA CAC CA	CAG GGA CTT CCC ATC CAC CT

TNF-α, tumor necrosis factor alpha; IL-1β, interleukin-1 beta; CINC-2, cytokine-induced neutrophil chemoattractant-2; MIP, macrophage inflammatory protein; MCP, monocyte chemoattractant protein; ICAM-1, intercellular adhesion molecule-1.

for 1 min for monocyte chemoattractant protein (MCP)-1; 30 cycles at 94 °C for 30 s, 56 °C for 1 min, and 72 °C for 1 min for MIP-1α; 30 cycles at 94 °C for 30 s, 60 °C for 1 min, and 72 °C for 1 min for MIP-1β; and 30 cycles at 94 °C for 45 s, 55 °C for 30 s, and 72 °C for 90 s for intercellular adhesion molecule (ICAM)-1. The housekeeping gene β-actin was used as the RT-PCR control, and its cycling program was 25 cycles at 94 °C for 30 s, 60 °C for 1 min, and 72 °C for 1 min. For every gene, the final cycle was followed by soaking for 7 min at 72 °C. RT-PCR products were analyzed using 2.0% agarose gel electrophoresis, and visualized by staining with ethidium bromide.

Statistical analysis

Differences among the groups were evaluated by the Mann–Whitney *U*-test. All values are expressed as mean ± SEM, and data were considered significant at $P < 0.05$.

Results

Serum ALT levels at 1, 3, 6 and 24 h after reperfusion

The serum ALT levels in each group are shown in Fig. 2. Among the groups that underwent ischemia–reperfusion, ALT increased to 11207 ± 1957 U/l in group C-6, but decreased to 3782 ± 1334 U/l in group M-6, which was significantly lower than the level in group C-6. The effect of MCI-186 became less prominent 24 h after reperfusion.

Consequently, we focused on changes occurring 24 h after reperfusion. The ALT levels were 5445 ± 1155 U/l (group C-24) vs. 4405 ± 1387 U/l (group M-24). However, additional administration of MCI-186 at 12 h after reperfusion markedly inhibited the increase in ALT levels to 1065 ± 605 U/l (group MX-24).

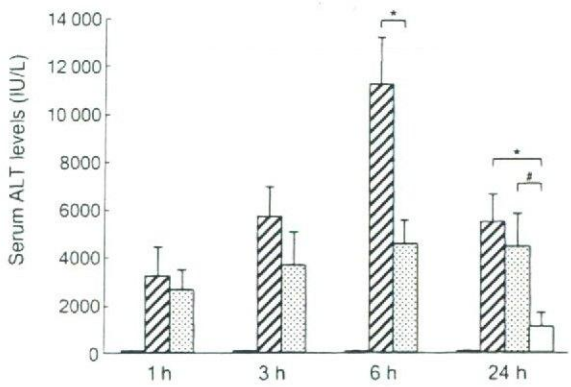

Figure 2 Effects of MCI-186 on serum alanine aminotransferase (ALT) levels. In the acute phase, rats treated with MCI-186 (group M) had lower ALT levels than the saline-treated group (group C). The ALT level in group MX-24 was significantly lower than that in groups C-24 and M-24. Values are expressed as mean ± SEM. *$P < 0.05$ compared with group C; #$P < 0.05$ compared with group M-24. ■, group S; ▨, group C; □, group M; □, group MX.

Histologic analysis

No pathologic findings were observed in the liver tissues of the sham control groups (data not shown). In group C-6, liver specimens exhibited focal necrosis, sinusoidal congestion and infiltration of leukocytes, and these changes became more severe in group C-24 (Fig. 3). In contrast, such findings were minimal in group M-6, but were observed in group M-24. In group MX-24, pathologic findings of spotty necrosis, sinusoidal congestion and infiltration of leukocytes were minimal compared with groups C-24 and M-24. These results were confirmed by a semi quantitative assessment, and shown to be significant (Table 2).

Immunohistochemistry for 4-HNE detection

There were no 4-HNE-positive cells in the liver in the sham control groups (data not shown). In groups C-6 and C-24, 4-HNE-positive cells were observed, but the 4-HNE levels were demonstrably reduced in group M-6 (Fig. 4). The number of 4-HNE-positive cells was lower in group MX-24 than in groups C-24 and M-24.

Immunohistochemistry for infiltrating cells

The numbers of cells positive for ED-1 (free macrophages) and ED-2 (resident macrophages) in the ischemic lobes were increased in group C-6, but not in group M-6 (Fig. 5a and b). However, such cells were increased to some extent in group M-24. In group MX-24, the numbers of both ED-1 and ED-2 positive cells were markedly reduced in comparison with groups C-24 and M-24. Figure 5c shows a similar tendency of infiltrated neutrophils into the sinusoids.

Expression of cytokine and chemokine mRNAs

Expression of cytokine and chemokine genes in the ischemic hepatic lobes in groups C and M was compared with that in group S, the sham control group (Fig. 6a). Expression of TNF-α mRNA was high after 1 h (group C-1) and then gradually decreased with time, and was lower in group M-1 than in group C-1 (Fig. 6b). Expression of IL-1 mRNA was high in groups C-1, C-3 and C-6, but attenuated in groups M-3 and M-6. The expression levels of CINC-2 (rat IL-8), MIP-2, MCP-1, MIP-1α and MIP-1β mRNAs were increased in groups C-3 and

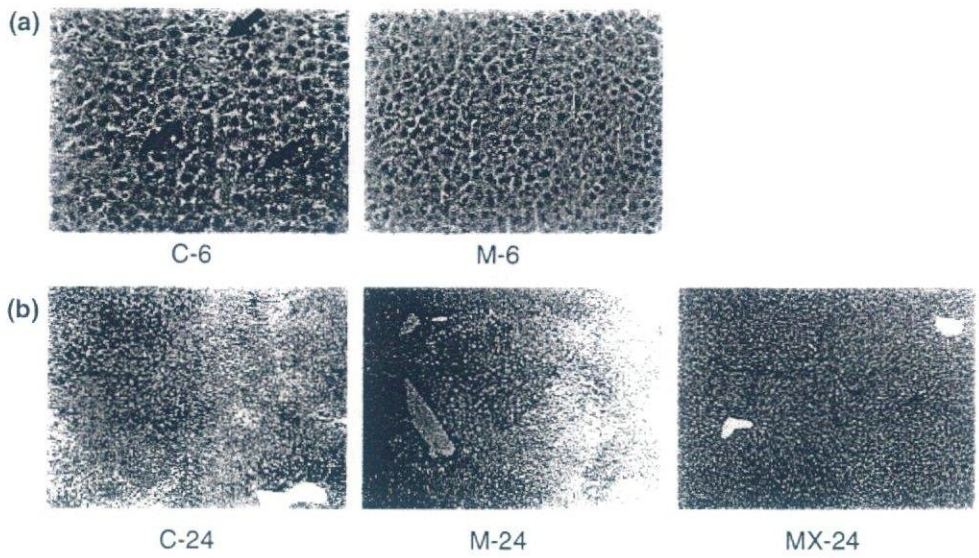

Figure 3 Representative histologic findings in the excised livers at 6 h and 24 h after reperfusion. (a) At 6 h after reperfusion, focal necrosis (arrows) and sinusoidal congestion were observed in the control group (group C-6) but not in the MCI-186-treated group (group M-6). Original magnification ×400. (b) At 24 h after reperfusion, spotty necrosis, ballooning of parenchymal cells, and more severe sinusoidal congestion were seen in the control group (group C-24) and also in the MCI-186-treated group (group M-24) but not in group MX-24 (original magnification ×100).

Table 2. Numerical degree of histologic damage according to the criteria advocated by Suzuki *et al.* (28). Congestion, vacuolization, and necrosis in liver tissue were estimated.

Groups	Congestion	Vacuolization	Necrosis
C-6	3.67 ± 0.21	0.67 ± 0.21	3.33 ± 0.21
M-6	2.33 ± 0.33*	0.50 ± 0.22	2.33 ± 0.21*
C-24	3.17 ± 0.17	3.50 ± 0.22	3.83 ± 0.17
M-24	2.83 ± 0.17	2.33 ± 0.21*	3.67 ± 0.21
MX-24	1.67 ± 0.21*,**	1.83 ± 0.31*	2.50 ± 0.22*,**

*$P < 0.05$ compared with group C.
**$P < 0.05$ compared with group M-24.

C-6, but those of the mRNAs for chemokines CINC-2, MIP-2, MCP-1 and MIP-1α were significantly decreased in group M-6. Expression of MIP-1β mRNA was not suppressed by MCI-186 at any time point. Figure 6c shows the expression of cytokine and chemokine mRNAs at 24 h. Expression was still high in group C-24, and CINC-2 and MIP-2 mRNA expression was suppressed significantly in group M-24. However, no suppression of IL-1, MCP-1, MIP-1α, and MIP-1β mRNA expression was evident. In group MX-24, the expression levels of mRNAs for all cytokines and chemokines were low. The differences in the expression levels of IL-1, MCP-1, MIP-1α and MIP-1β mRNAs were significant in comparison with groups C-24 and M-24.

We also investigated ICAM-1 mRNA expression at 6 h, as shown in Fig. 7. ICAM-1 mRNA expression was high 6 h after reperfusion (group C-6) and gradually decreased thereafter. The expression was significantly reduced in group M-6.

Discussion

We have investigated the usefulness of MCI-186 for the prevention of hepatic warm IRI in a rat model. The results demonstrate that administration of MCI-186 before reperfusion suppressed IRI in the acute phase, but did not result in sufficient suppression in the subacute phase. Additional administration of MCI-186 12 h after reperfusion also suppressed IRI in the subacute phase. This additional administration is presumably necessary because of the short half-life of MCI-186 and the multistep nature of hepatic IRI [1–9].

Free radicals are one of the important factors responsible for hepatic IRI [2–5,29], and several investigators have reported that free radical scavengers attenuate hepatic IRI [3–5,30–35]. Nevertheless, no such scavenger has been used clinically to date recently. MCI-186 is now used clinically and is beneficial after cerebral infarction. There have been several reports describing beneficial effect of MCI-186 on hepatic IRI, e.g. it attenuates liver injury at acute phase [22], it protects against mitochondrial injury [23] and it ameliorates cold IRI [20] or warm IRI [21] in isolated liver perfusion model using Krebs–Henseleit solution. However, none of these studies have focused on the effects of this reagent against various chemical

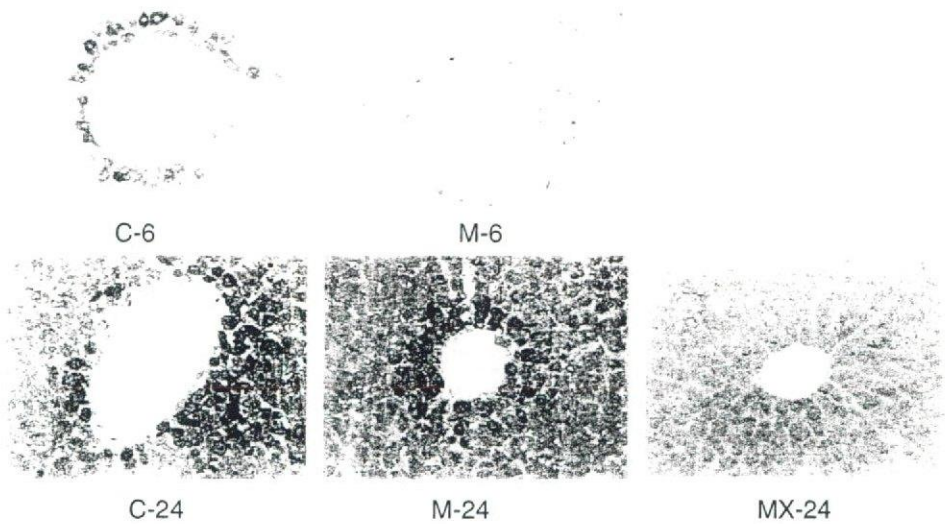

Figure 4 Representative findings of lipid peroxidation immunostaining with monoclonal antibody against 4-hydroxy-2-nonenal (4-HNE) modified proteins in rat livers at 6 h and 24 h after reperfusion. In groups C-6 and C-24, 4-HNE-positive cells were observed. Although 4-HNE staining was faint in group M-6, the number of 4-HNE-positive cells in group M-24 was comparable with that in group C-24. The number of 4-HNE-positive cells was decreased in group MX-24, compared with groups C-24 and M-24 (original magnification ×400).

mediators such as free radicals, cytokines and chemokines, inflammatory cells, adhesion molecules, and also against histologic damage in hepatic IRI model *in vivo*.

The ODFRs activate monocytes (resident or free) and induce nuclear factor κB in hepatic IRI, causing hepatic injury in the early phase [8,12,31,36–38]. TNF-α and IL-1β are potent proinflammatory cytokines secreted mainly by Kupffer cells during hepatic IRI [2–6,8,39,40]. These cytokines induce IL-8 and CINC-2 synthesis [4,41] and upregulate the expression of adhesion molecules such as Mac-1 or ICAM-1 [3,4]. TNF-α also induces chemokines such as epithelial neutrophil-activating protein 78, which plays an important role in neutrophil chemotaxis and activation, and stimulates ODFR production by Kupffer cells [2,4,7,42,43]. IL-1β induces Kupffer cells to produce TNF-α, upregulates ODFR production by neutrophils [4], and also upregulates the expression of nuclear factor κB and CXC chemokines [8]. In this study, the expression of TNF-α and IL-1β was elevated in the early phase after reperfusion, and attenuated in the MCI-186-treated groups.

MCP-1, MIP-1α and MIP-1β are CC chemokines, which exert a chemotactic effect on monocytes and T cells [10–13]. The expression levels of MCP-1 and MIP-1α were reduced in the MCI-186-treated group 3 h and 6 h (acute phase) after reperfusion. MCI-186 reduced monocyte infiltration into the liver, and this might have resulted from suppressed expression of CC chemokines. In the early phase of hepatic IRI, ODFR-stimulated Kupffer cells release MCP-1 [12], upregulates ICAM-1 expression on endothelial cells *in vitro* [44]. Up-regulation of ICAM-1 is one of the important factors involved in the pathogenesis of neutrophil-induced hepatic IRI [45]. These correlations appear to be supported by the present *in vivo* data indicating that suppression of MCP-1 and ICAM-1 expression in the MCI-186-treated groups led to a decrease in monocyte and neutrophil infiltration.

Similar mRNA expression patterns were also observed for members of the CXC chemokine superfamily (CINC-2 and MIP-2). CXC chemokines have potent chemotactic effects on neutrophils. Kupffer cells produce CINC when stimulated with ODFR generated by hypoxanthine and xanthine oxidase [2,3,41], while CINC-2 production can be reduced with a calcium channel blocker [41]. The level of CINC-2 is increased for several hours after reperfusion in rat liver IRI models [2,41]. MIP-2 is also upregulated in early hepatic or renal IRI and has an important role in neutrophil recruitment and organ injury [7,9,13]. Our results indicate that CINC-2 and MIP-2 levels were elevated in the early phase of IRI in the control groups, and we suspect a correlation between the expression of CXC chemokines and neutrophil infiltration. This inference is supported by the observation that both CXC chemokine expression and neutrophil infiltration were suppressed in the MCI-186-treated groups.

In our study, single administration of MCI-186 did not have attenuated infiltration of neutrophils or macrophages in the subacute phase presumably because of its short

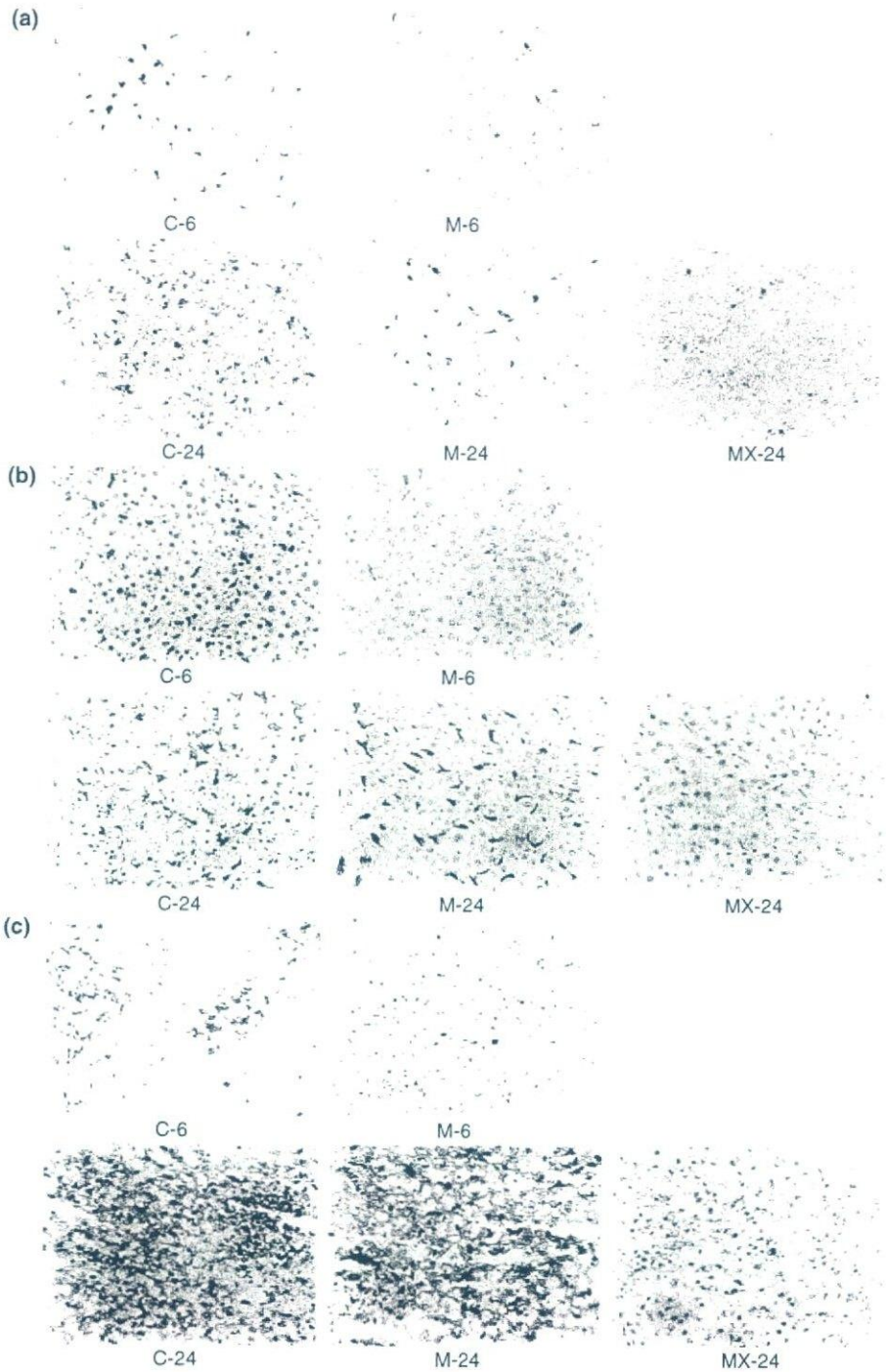

Figure 5 Immunohistochemistry for inflammatory cells in the liver tissues. (a) ED-1-positive cells (resident macrophages). (b) ED-2-positive cells (free macrophages). (c) Neutrophils. The numbers of ED-1- and ED-2-positive cells in the ischemic lobes were increased in group C-6 but absent in group M-6. In group M-24, the numbers of ED-1- and ED-2-positive cells in the ischemic lobes were increased. In group MX-24, the number of macrophages was markedly reduced. Infiltration of neutrophils into the sinusoids was observed in groups C-6 and C-24. Infiltration was suppressed in group M-6, but not in group M-24. In group MX-24, infiltration of neutrophils into sinusoids was demonstrably reduced (original magnification ×400).

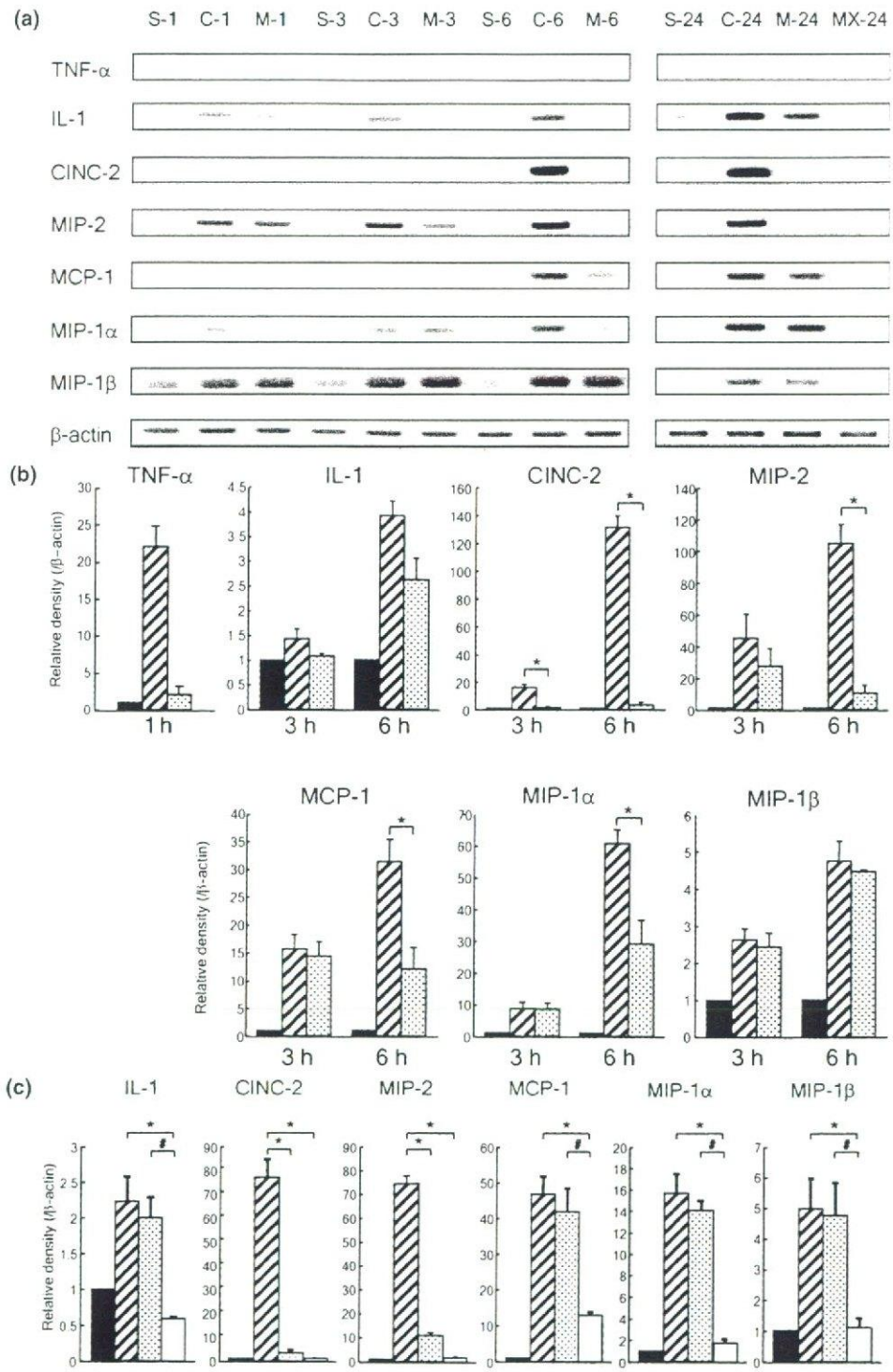

Figure 6 (a) Expression of cytokine and chemokine mRNAs in ischemic lobes of rats. (b) Semiquantification of cytokines and chemokines in the acute phase. (c) Semiquantification of cytokine and chemokines in the subacute phase. Analysis of bands for β-actin and cytokines or chemokines is shown, and the data represent the ratio from five different animals. The expression of cytokines and chemokines was high in group C, but attenuated in group M and group MX. Data represent mean ± SEM. $*P < 0.05$ compared with group C; $\#P < 0.05$ compared with group M-24. ■, group S; ▨, group C; ▨, group M; □, group MX.

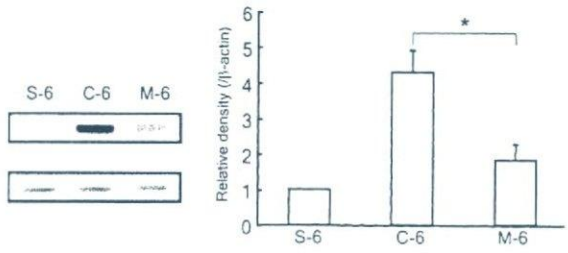

Figure 7 Level of expression of intercellular adhesion molecule (ICAM)-1 mRNA in the ischemic lobe at 6 h after reperfusion. Analysis of bands for ICAM-1 and β-actin is shown, and the data represent the ratio from five different animals. The expression of ICAM-1 was high in group C, but attenuated in group M. Data represent mean ± SEM. $*P < 0.05$ compared with group C.

half-life and the timing of injection [the half-life of MCI-186 is 0.17 h ($t_{1/2}\alpha$) and 0.81–0.85 h ($t_{1/2}\beta$) at a dose of 1.5 mg/kg in clinical laboratory tests] [27]. These pharmacokinetic data suggested the need for a second experiment that included additional administration of MCI-186 (group MX-24). As a result, additional administration of MCI-186 at 12 h after reperfusion suppressed IRI with attenuation of ODFRs and other mediators in the subacute phase.

In summary, MCI-186 attenuates liver injury *in vivo* in a rat warm IRI model, suggesting that this clinically applicable free radical scavenger has the potential to attenuate liver dysfunction in patients after hepatic resection and liver transplantation.

Acknowledgements

This work was supported in part by a grants-in-aid for scientific research from the Ministry of Education, Culture, Sports, Science and Technology of Japan (08457297, 09877243, 13470150), the Takeda Medical Foundation, and the Vehicle Racing Commemorative Foundation. We would like to thank Ms K. Misawa for technical assistance.

References

1. Jaeschke H, Farhood A, Smith CW. Neutrophils contribute to ischemia/reperfusion injury in rat liver *in vivo*. *FASEB J* 1990; **4**: 3355.
2. Teoh NC, Farrell GC. Hepatic ischemia reperfusion injury: pathogenic mechanisms and basis for hepatoprotection. *J Gastroenterol Hepatol* 2003; **18**: 891.
3. Jaeschke H. Molecular mechanisms of hepatic ischemia–reperfusion injury and preconditioning. *Am J Physiol Gastrointest Liver Physiol* 2003; **284**: G15.
4. Serracino-Inglott F, Habib NA, Mathie RT. Hepatic ischemia–reperfusion injury. *Am J Surg* 2001; **181**: 160.
5. Fondevila C, Busuttil RW, Kupiec-Weglinski JW. Hepatic ischemia/reperfusion injury – a fresh look. *Exp Mol Pathol* 2003; **74**: 86.
6. Zwacka RM, Zhang Y, Halldorson J, Schlossberg H, Dudus L, Engelhardt JF. CD4(+) T-lymphocytes mediate ischemia/reperfusion-induced inflammatory responses in mouse liver. *J Clin Invest* 1997; **100**: 279.
7. Lentsch AB, Yoshidome H, Cheadle WG, Miller FN, Edwards MJ. Chemokine involvement in hepatic ischemia/reperfusion injury in mice: roles for macrophage inflammatory protein-2 and KC. *Hepatology* 1998; **27**: 1172.
8. Kato A, Gabay C, Okaya T, Lentsch AB. Specific role of interleukin-1 in hepatic neutrophil recruitment after ischemia/reperfusion. *Am J Pathol* 2002; **161**: 1797.
9. Martinez-Mier G, Toledo-Pereyra LH, McDuffie JE, Warner RL, Ward PA. Neutrophil depletion and chemokine response after liver ischemia and reperfusion. *J Invest Surg* 2001; **14**: 99.
10. Luster AD. Chemokines–chemotactic cytokines that mediate inflammation. *N Engl J Med* 1998; **338**: 436.
11. Baggiolini M. Chemokines and leukocyte traffic. *Nature* 1998; **392**: 565.
12. Yamaguchi Y, Matsumura F, Liang J, *et al.* Neutrophil elastase and oxygen radicals enhance monocyte chemoattractant protein-1 expression after ischemia/reperfusion in rat liver. *Transplantation* 1999; **68**: 1459.
13. Martinez-Mier G, Toledo-Pereyra LH, McDuffie JE, *et al.* Exogenous nitric oxide down-regulates MIP-2 and MIP-1 α chemokines and MAPK p44/42 after ischemia and reperfusion of the rat kidney. *J Invest Surg* 2002; **15**: 287.
14. Rabb H, Daniels F, O'Donnell M, *et al.* Pathophysiological role of T lymphocytes in renal ischemia–reperfusion injury in mice. *Am J Physiol Renal Physiol* 2000; **279**: F525.
15. Anselmo DM, Amersi FF, Shen XD, *et al.* FTY720 pretreatment reduces warm hepatic ischemia reperfusion injury through inhibition of T-lymphocyte infiltration. *Am J Transplant* 2002; **2**: 843.
16. Abe K, Yuki S, Kogure K. Strong attenuation of ischemic and postischemic brain edema in rats by a novel free radical scavenger. *Stroke* 1988; **19**: 480.
17. Houkin K, Nakayama N, Kamada K, Noujou T, Abe H, Kashiwaba T. Neuroprotective effect of the free radical scavenger MCI-186 in patients with cerebral infarction: clinical evaluation using magnetic resonance imaging and spectroscopy. *J Stroke Cerebrovasc Dis* 1998; **7**: 315.
18. Tohgi H, Kogure K, Hirai S, *et al.* Effect of a novel free radical scavenger, Edaravone (MCI-186), on acute brain infarction. *Cerebrovasc Dis* 2003; **15**: 222.
19. Nishi H, Watanabe T, Sakurai H, Yuki S, Ishibashi A. Effect of MCI-186 on brain edema in rats. *Stroke* 1989; **20**: 1236.
20. Ninomiya M, Shimada M, Harada N, Soejima Y, Suehiro T, Maehara Y. The hydroxyl radical scavenger MCI-186